Additions to Voyager 2 Cosmic Ray Subsystem Data from the Uranus and Neptune Flybys in the Planetary Data System's Planetary Plasma Interactions Node

Funded by NASA ROSES PDART Grant 80NSSC20K0550, PI M. D. Looper

December 30, 2024

Contents

1. PDS/PPI Data Holdings from Voyager 2 CRS at Uranus and Neptune 2
1.1. Present Status 2
1.2. Additions From This Project 2
1.2.1. CRS Operating Modes and Countrates 3
1.2.2. Countrate Definitions, Particle and Energy Response 6
2. Data File Contents 9
2.1. Proton Fluxes at Neptune 9
2.2. Six-Second Countrates at Uranus and Neptune 11
2.2.1. Timing Irregularities in the Uranus Countrates 12
2.3. Several Countrates at Lower Time Resolution from Neptune 12
2.3.1. Timing of the Neptune Data 13
3. References 14
Appendix A. History of This Augmentation Project and Provenance of Data 14
Appendix B. Plots of Six-Second Neptune Countrates 17
Appendix C. Scanned Original Documents 34

© The Aerospace Corporation, 2024
Approved for public release. OTR-2025-00328.

1. PDS/PPI Data Holdings from Voyager 2 CRS at Uranus and Neptune

1.1. Present Status

The Cosmic Ray Subsystem (CRS) aboard the two Voyager spacecraft consists of seven solid-state detector telescopes: four Low Energy Telescopes (LETs) labeled A through D, two High Energy Telescopes (HETs) labeled 1 and 2, and a single Electron Telescope (TET). The Voyager 2 spacecraft flew by Uranus in 1986 and Neptune in 1989, and all CRS sensors returned data throughout each encounter. The Planetary Plasma Interactions node of NASA's Planetary Data System (PDS/PPI) is the standard repository for space radiation data from the planets, but to date its only holdings of the CRS measurements at each of these encounters are tabulations at 96-second resolution of countrates from the D1 and D2 detectors of TET and, at Neptune, a 6-second tabulation of a brief subset (~12 minutes) of the TET D1 countrate. A summary of these PDS/PPI holdings, assembled by R. Selesnick in the early 1990s, is given in Table 1.

Table 1

Planet	Det.	Res.	Bundle ID	DOI
Uranus	D1	96 sec	VG2-U-CRS-4-SUMM-D1-96SEC-V1.0	10.17189/1520021
Uranus	D2	96 sec	VG2-U-CRS-4-SUMM-D2-96SEC-V1.0	10.17189/1520022
Neptune	D1	6 sec	VG2-N-CRS-3-RDR-D1-6SEC-V1.0	10.17189/1519963
Neptune	D1	96 sec	VG2-N-CRS-4-SUMM-D1-96SEC-V1.0	10.17189/1519964
Neptune	D2	96 sec	VG2-N-CRS-4-SUMM-D2-96SEC-V1.0	10.17189/1519965

Table 1: Present holdings of PDS/PPI from Voyager 2 CRS at Uranus and Neptune.

1.2. Additions From This Project

In the course of the present project, we collected and organized two major subsets of CRS data for submission to PDS/PPI: calibrated proton fluxes from LET C and LET D at Neptune, and numerous raw countrates from all sensors during the Uranus and Neptune flybys. The latter include a selection of single-detector and coincidence countrates from all CRS sensors, taken from the encyclopedia files at NASA's Goddard Space Flight Center (GSFC) preserved by N. Lal. The proton fluxes were from the PhD thesis research of the PI of this project (Looper, 1993); we also provide a few Neptune TET and LET countrates obtained from the records of that research because, although some of them were at lower time resolution than is available in the main GSFC-derived dataset (6-second rates averaged over 96 seconds), they fill in some data gaps in the time series extracted from the GSFC files. In particular, we do not have any countrates from the earliest part of the Voyager 2 encounter with Neptune's magnetosphere on day 236 of 1989 in the GSFC data, and the thesis countrate files included the last four hours of that day.

1.2.1. CRS Operating Modes and Countrates

In Section 2 we will describe the contents of all the files that compose our PDS/PPI submission; here we list the rates that were extracted from the GSFC files for a portion of the submission, which are a subset of all the rates returned in the Voyager telemetry. All such countrates are accumulated in 6-second intervals, but some rates are tabulated every six seconds while others are "subcommutated," with a single rate scaler shared among up to sixteen different countrates in a 96-second rotation. In addition, LET C, LET D, and HET 1 toggled between two operating modes during both encounters. The HET sensors have high- and low-gain modes; HET2 remained in low-gain mode during the entirety of both encounters, while HET1 switched between these modes every 192 seconds. LET C and LET D switched between "doubles" and "triples" modes every 192 seconds, which means that the coincidence condition required for a particle event in LET C or LET D to trigger pulse-height analysis (PHA) and inclusion in the telemetry stream required only the L1 and L2 detectors of that LET for doubles mode, and required L1, L2, and L3 in triples mode. This ensured that higher-energy protons that triggered all three detectors would not be crowded out of the PHA-event queue by the much more abundant lower-energy protons that only triggered the first two detectors. HET 1 was in high-gain mode when LET C and LET D were in doubles mode, and in low-gain mode when they were in triples mode. The two (combined) modes will be referred to hereinafter as H2 and L3; they were not arranged in a simple alternation, but rather were repeated on a cycle of 15 x 192 seconds (48 minutes), as L3/H2/L3/H2/L3/H2/L3/H2/L3/H2/L3/H2/L3/H2/L3 with L3 repeating at the start and end of each such interval.

Table 2 lists all the countrates available in the Voyager telemetry, with those that we are providing for both the Uranus and Neptune encounters highlighted in green, while a few HET1 coincidence rates that we were only able to obtain for the Neptune encounter are highlighted in yellow. The columns in the table are (1) the sensor for the rate listed in each row; (2) the counter in which the rate is accumulated, numbered 1-30 with counter 27 not used; (3) the subcommutator state or states during which the rate is accumulated, numbered 0-15; (4) the label of the rate accumulated in that counter and subcom state during H2 mode; and (5) the label of the rate accumulated during L3 mode. These specifications are taken from file "ratesTable.c" of N. Lal (see discussion of provenance in Appendix A) and are consistent with tables in the CRS Science Requirements Document (Garrard, revised 1978). Note that LCX2, LCX3, LDX2, and LDX3 are not standard Voyager notation, as in the SRD; these are subsets of the LCZ3* and LDZ3* PHA-analysis-trigger rates, which we used to separate the LET C and LET D data in doubles mode from that in triples mode for our PDS/PPI data submission. Note also that the "H" or "L" on the various TET single-detector rates denotes high or low discriminator thresholds that could be triggered simultaneously, not high or low gain modes that were toggled between, as for the HETs.

Table 2

Sensor	Counter	Subcom State(s)	Rate in H2 Mode	Rate in L3 Mode
HET 1	1	ALL	IAS	IASZ3
	2	0-2, 4-6, 8-10, 12-14	IBSp	IBSZ2
		3, 7, 11, 15	IBSe	
	3	ALL	IPENH	IPENL
	4	ALL	IPGH	IPGL
	5	EVEN	IBS4p	IBS4Z2
		ODD	IBS4e	IBS4
	6	EVEN	IBS3p	IBS3Z2
		ODD	IBS3e	IBS3
	7	EVEN	IBS2p	IBS2Z2
		ODD	IBS2e	IBS2
	8	0	IA1H	IA1L
		1	IA2H	IA2L
		2	IC1H	IC1L
		3	IC2H	IC2L
		8	IC3H	IC3L
		9	IC4H	IC4L
		10	IB2H	IB2L
		11	IG1	IG1
		4, 12	IB1H	IB1L
		5, 13	ISA1H	ISA1L
		6, 14	ISA2H	ISA2L
		7, 15	ISBH	ISBL
HET 2	9	ALL	IIAS	IIASZ3
	10	0-2, 4-6, 8-10, 12-14	IIBSp	IIBSZ2
		3, 7, 11, 15	IIBSe	
	11	ALL	IIPENH	IIPENL
	12	ALL	IIPGH	IIPGL
	13	EVEN	IIBS4p	IIBS4Z2
		ODD	IIBS4e	IIBS4
	14	EVEN	IIBS3p	IIBS3Z2
		ODD	IIBS3e	IIBS3
	15	EVEN	IIBS2p	IIBS2Z2
		ODD	IIBS2e	IIBS2
	16	0	IIA1H	IIA1L
		1	IIA2H	IIA2L
		2	IIC1H	IIC1L

		3	IIC2H	IIC2L
		8	IIC3H	IIC3L
		9	IIC4H	IIC4L
		10	IIB2H	IIB2L
		11	IIG1	IG1
		4, 12	IIB1H	IIB1L
		5, 13	IISA1H	IISA1L
		6, 14	IISA2H	IISA2L
		7, 15	IISBH	IISBL
LET A	17	ALL	LAZ3*	
	18	ALL	LAZ3	
LET B	19	ALL	LBZ3*	
	20	ALL	LBZ3	
LET C	21	ALL	LCX2	LCX3
	22	ALL	LCZ3	
LET D	23	ALL	LDX2	LDX3
	24	ALL	LDZ3	
LET A	25	0	LA1	
		1	LA2	
		2	LA3	
		3	LA4	
		4, 12	SLA	
LET B		5, 13	SLB	
LET A		6, 14	LATRP	
LET B		7, 15	LBTRP	
		8	LB1	
		9	LB2	
		10	LB3	
		11	LB4	
LET C	26	0	LC1	
		1	LC2	
		2	LC3	
		3	LC4	
		4, 12	SLC	

LET D		5, 13	SLD	
LET C		6, 14	LCTRP	
LET D		7, 15	LDTRP	
		8	LD1	
		9	LD2	
		10	LD3	
		11	LD4	
TET	28	ALL	TAN	
	29	EVEN	TLO	
		ODD	THI	
	30	0	D6L	
		1	GA+GB	
		2	D5H	
		3	D7L	
		4	D6H	
		5	D7H	
		6	D5L	
		7	D8L	
		8	D1H	
		9	D4H	
		10	D2L	
		11	D3L	
		12	D1L	
		13	D3H	
		14	D2H	
		15	D4L	

Table 2: Accumulation parameters for CRS rates, with those included in the PDS/PPI data submission highlighted green if present for both encounters, yellow for Neptune only.

1.2.2. Countrate Definitions, Particle and Energy Response

The proton fluxes are scrubbed of background, corrected for detector deadtime, and split into eight energy channels from 1.9 to 7.8 MeV for each of LET C and LET D using countrates and PHA data as described by Looper (1993). The countrates that compose the rest of our data submission are defined only by energy-deposit thresholds and/or by requirements that certain detectors' energy-deposit thresholds be exceeded in the same particle event; thus there is less information available to determine the particles and energy ranges to which each responds. Estimates are available, however, and in Table 3 and 4 we reproduce, with permission, some information from the notebooks of A. Cummings.

Table 3 shows the definitions of the coincidence rates during the Uranus encounter, which were modified from the definitions used during interplanetary cruise as enumerated by Garrard (1978). In particular, most guard anticoincidence requirements were deleted in order that real events not be suppressed if guard countrates in the planets' unknown magnetospheric environments were too high. It also shows estimates of the particles and energy ranges to which each coincidence rate responds, and of the effective geometry factor for each. The coincidence requirements at the Neptune encounter were the same, except that around the closest approach to the planet, from about 0250 to 0510 on day 237 of 1989, the TAN (TET PHA analysis trigger) rate was changed from responding to all particle events triggering D1 to responding to all events triggering D4 (Stone et al., 1989).

Table 3

Counting Rate Coincidence Equations for Format B:
(Detectors are identified by name. Sxx are slant discriminators)

Rate*	Name	Coincidence Condition	Species	Energy Range	G (cm^2 sr)
HET 1 counting rates					
R1	AS	A1.A2.C4*.B2*	protons	> 4 MeV	1.24
R2a	BSp	B1.B2.C1*.A2*.SB1	protons	> 18 MeV	1.69
R2b	BSe	B1.B2.C4.C1*.A2*.SB1*	electrons	> 2.6 MeV	1.46
R3	PEN	B1.B2.C1	protons	> 70 MeV	1.65
R4	PEN.G1*	B1.B2.C1	electrons	> 12 MeV	1.65
R5a	BS4e	B1.B2.C4.C3*.SB1*	electrons	2.6 – 5.1 MeV	1.46
R5b	BS4p	B1.B2.C4.C3*.SB1	protons	27 – 48 MeV	1.46
R6a	BS3e	B1.B2.C4.C3.C2*.SB1*	electrons	5.1 – 8 MeV	1.25
R6b	BS3p	B1.B2.C4.C3.C2*.SB1	protons	48 – 63 MeV	1.25
R7a	BS2e	B1.B2.C4.C3.C2.SB1*	electrons	> 8 MeV	0.96
R7b	BS2p	B1.B2.C4.C3.C2.SB1	protons	> 63 MeV	0.96
R8	various singles rates for HET 1				
HET 2 counting rates					
R9	ASZ3	zero (A1 off)			
R10	BSZ2	B2.SB2.A2*	Z ≥ 2 ions		
R11	PEN	B2	protons	> 20 MeV	25
R12	PEN.G1*	B2	electrons	> 2.5 MeV	25
R13a	BS4Z2*	B2.C4.C3*.SB2*	protons	27 – 48 MeV	20
R13b	BS4Z2	B2.C4.C3*.SB2	Z ≥ 2 ions		
R14a	BS3Z2*	B2.C4.C3.C2*.SB2*	protons	48 – 63 MeV	10.5
R14b	BS3Z2	B2.C4.C3.C2*.SB2	Z ≥ 2 ions		
R15a	BS2Z2*	B2.C4.C3.C2.SB2*	protons	63 – (160) MeV	6.5

R15b	BS2Z2	B2.C4.C3.C2.SB2	Z ≥ 2 ions	72 – (180) MeV	4.7
R16	various singles rates for HET 2				
LET counting rates (note that LETs C and D are cycled between L12 and L123).					
R17	LAZ*	L1.SLA*	protons	> 0.5 MeV	4.6
R18	LAZ	L1.SLA	Z > 2 ions		4.6
R19	LBZ*	zero (LB1 off)			
R20	LBZ	zero (LB1 off)			
R21	LCZ*	L1.L2.[L3].SLC* L12.SL*:	protons	1.8 – 3.0 MeV	0.49
R22	LCZ	L1.L2.[L3].SLC L12.SL:	Z > 2 ions		0.49
R23	LDZ*	L1.L2.[L3].SLD* L123.SL*:	protons	> 3.0 MeV	0.49
R24	LDZ	L1.L2[L3].SLD L123.SL:	Z > 2 ions		0.49
R25, R26 various singles rates for LETs					
TET counting rates					
R28	TAN	D1L.D1H*	electrons	≥ 0.6 MeV	14.
R29a	TLO	D1L.D1H*.D4H*.D5L.D5H*. D6L*.D6H*.D7H* (D1.D5.D6*)			
R29b	THI	D1L.D1H*.D4H*.D5H*.D6H* .D7L.D7H* (D1.D7)			
R30	various singles rates for TET				

Table 3: Coincidence definitions and responses during the Uranus encounter. The asterisk represents a logical NOT. In the Name column, for example, G1 means with no G1 (guard) trigger, and Z* and Z2* mean no ions heavier than photons (or possibly alphas for LET). In the Coincidence Condition column, it indicates that a threshold is required not to be triggered. A scanned copy of the original document is provided in Figure 19 (see Appendix C).*

Table 4 shows similar estimates of proton and electron response for some individual detectors' countrates, from a notebook page at the time of the Neptune encounter. Cooper and Stone (1991) provide more discussion of this in an appendix, and Stone et al. (1989) in a footnote.

Table 4

Preliminary CRS Thresholds and G-factors 8/24/89

System	Detector	AΩ (cm^2 sr)	electron E-thr	proton E-thr
LET	L1	4.6	pile-up	0.5
	L12	0.49	pile-up	1.8
	L123	0.49	pile-up	3
	L4		0.7	

HET	A1H	20	pile-up	0.2
	A2H	1.24	pile-up	4
	C1H	20		
	C2H	11.18	3.11	
	C3H	42.4	5.95	50
	C4H	20.48	3.1	30
	B2H	12.74	1.14	18
	B1H	25	0.5	
	A1L	off	off	off
	A2L	1.24	pile-up	4
	C1L	off	off	off
	C2L	13.31	8.47	
	C3L	30.2	10.26	50
	C4L	13.26	7.56	30
	B2L	25	3	20
	B1L	off	off	off
TET	D1L	11.24	1.09	upper thresh
	D2L			
	D3L			
	D4L			

Table 4: Estimates of proton and electron responses of various single-detector countrates. A scanned copy of the original document is provided in Figure 20 (see Appendix C).

2. Data File Contents

2.1. Proton Fluxes at Neptune

The proton fluxes are divided into eight energy bins for each of LET C and LET D: 1.9-2.1, 2.1-2.9, 3.2-3.7, 3.7-4.3, 4.3-5.0, 5.0-5.8, 5.8-6.7, and 6.7-7.8 MeV. The first two energy channels are in doubles mode and the rest are in triples mode, so the times are interleaved as described in Section 1.2.1. The data are collected into sixteen comma-separated value (CSV) files, one for each of the eight channels of the two LETs; filenames are "prot_X_YYY.csv," where X is "c" or "d" to indicate which LET the file is for and YYY is the midpoint of the energy channel in MeV with decimal point omitted.

For each of the proton flux files, the first line gives the LET and energy channel, the second gives column titles, and the remaining 105 or 120 lines for doubles and triples channels respectively give the time-ordered data. To obtain adequate statistics, each row of the data

accumulates the whole 192 seconds of a single period of H2 or L3 mode. A complete cycle of the sixteen steps of the subcommutator is referred to as a "volume," which during the Uranus and Neptune encounters was 96 seconds long, so each row of the data represents two volumes as labeled. The contents of the columns are as follows, with missing data indicated by a fill value of -99 (integer or decimal):

1) Vol 0: number of the first of the two volumes in the accumulation interval
2) Vol 1: number of the second of the two volumes in the accumulation interval
3) Time: midpoint of the two-volume interval as *YYYY-MO-DD*T*HH*:*MM*:*SS*
4) Time start: start time of the two-volume interval as *YYYY-MO-DD*T*HH*:*MM*:*SS*
5) Time stop: end time of the two-volume interval as *YYYY-MO-DD*T*HH*:*MM*:*SS*
6) Hour: midpoint of the two-volume interval as decimal hours of 8/25/1989 (negative values for the two hours of data from 8/24/1989 at the start of each file)
7) Hour start: start time of the two-volume interval as decimal hours of 8/25/1989
8) Hour stop: end time of the two-volume interval as decimal hours of 8/25/1989
9) Counts: number of PHA events in this LET and energy channel during the interval
10) One-count flux: flux in units of protons per (cm^2 sr sec MeV) represented by one proton count during the data accumulation interval, accounting for geometry factor, accumulation time, energy channel width, and deadtime correction
11) log flux: log10 of flux measurement in units of protons per (cm^2 sr sec MeV) for the accumulation interval – if N is the number of counts and F is the one-count flux from the previous two columns, then this measurement is F * N, with the log of zero flux for N = 0 indicated by a -10 in this column
12) log flux low: log10 of one-sigma lower limit to flux measurement in units of protons per (cm^2 sr sec MeV) for the accumulation interval – if N > 0 then this is F * (N - sqrt(N - 0.25)), with a lower limit of the log of zero flux indicated by -10
13) log flux high: log10 of one-sigma upper limit to flux measurement in units of protons per (cm^2 sr sec MeV) for the accumulation interval – F * (N + 1 + sqrt(N + 0.75))
14) S/C L: L value for particles mirroring at the spacecraft location at the midpoint time of the data accumulation interval
15) S/C L start: L value for particles mirroring at the spacecraft location at the beginning of the data accumulation interval
16) S/C L stop: L value for particles mirroring at the spacecraft location at the end of the data accumulation interval
17) G/C L: L value for guiding center of protons at the midpoint energy of this channel coming down the sensor's boresight at the midpoint time of the interval
18) G/C L start: L value for guiding center of protons at the midpoint energy of this channel coming down the sensor's boresight at the beginning of the interval
19) G/C L stop: L value for guiding center of protons at the midpoint energy of this channel coming down the sensor's boresight at the end of the interval

Figure 1 shows a sample of this data scanned from a plot in the PI's files.

Figure 1

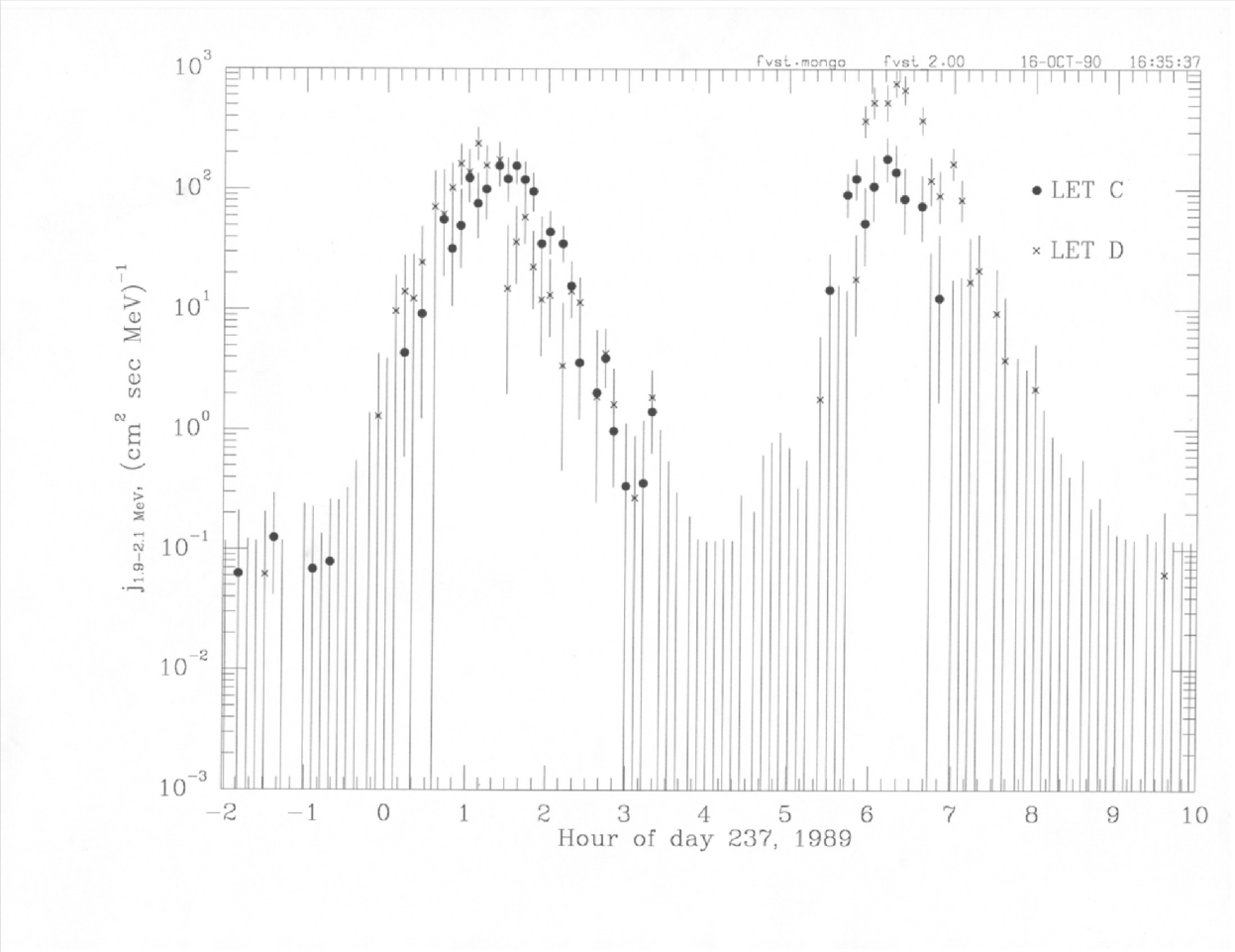


Figure 1: 1.2-2.1 MeV proton fluxes at Neptune as measured by LET C and LET D.

2.2. Six-Second Countrates at Uranus and Neptune

The single-detector and coincidence countrates highlighted in Table 2 are collected into a single CSV file for each planet named "rates_6sec_X.csv", where X is "u" or "n" for Uranus or Neptune respectively. Each file has one header line giving column labels, followed by a row for each 6-second period for which we were able to extract data from the GSFC holdings. Times run from 00:00 to 23:30 UT on day 24 of 1986 for Uranus, and from 00:00 to 19:30 on day 237 of 1989 for Neptune, with some gaps. The contents of the files' columns are (1) the time at the start of the 6-second accumulation interval; (2) the mode as described in Section 1.2.1, with a 0 indicating the H2 mode and a 1 indicating the L3 mode; (3) the subcom state from 0 to 15, as also described in Section 1.2.1; and (4 to end) the number of counts per 6-second accumulation interval in each of the countrates highlighted in Table 2. A fill value of -2 indicates that the countrate for a given column does not return data during the mode and subcom state for the time in a given row, while a fill value of -1 indicates that the countrate was expected to contain data in that row but it was either missing or invalid. Note that no "despiking" has been done, so that a few invalid data points in the form of outliers have not

been suppressed; a -1 fill value indicates that the files retrieved from GSFC did not have data for the given entry, rather than that we removed it. See Appendix B for plots of many of these countrates from the Neptune encounter.

2.2.1. Timing Irregularities in the Uranus Countrates

The sequence of timestamps was orderly for the Neptune data, in that all of them are 5 seconds plus a multiple of 6 seconds, even across data gaps. At Uranus, however, the timestamps jumped back and forth briefly (gaps of … 6, 6, 7, 5, 6, 6 …) at 30432 and 30624, and jumped forward permanently at 29861 (gaps of … 6, 6, 5, 6, 6 …) resulting in an offset for the remainder of the day. These jumps are understandable in the context of round off error if the spacecraft and sensor clocks are not perfectly synchronized. More confusingly, the timestamps are separated by 8 rather than 6 seconds from 10272 to 10656 and by 9 seconds from 43496 to 44063, though there is no evidence from the rates that the accumulation times actually changed from 6 seconds. For both Uranus and Neptune we were able to assign modes and subcom values in orderly sequences consistent with the patterns detailed in Section 1.2.1 These remained coherent throughout the Neptune dataset (records with the same subcom value have timestamps that are a multiple of 96 seconds apart, while the 15 x 192 second sequence of mode changes remained synchronized across data gaps), while the same is true at Uranus after adjustment for the one-second timing glitches, except for the brief spans when the timestamps were separated by 8 or 9 seconds rather than 6. We have left the timestamps as they came to us in the GSFC data, rather than impose corrections for either the one-second glitches or the anomalous separations.

2.3. Several Countrates at Lower Time Resolution from Neptune

In the course of searching through the PI's old Neptune data for the proton fluxes (see Appendix A), we found some files that collected several of the countrates highlighted in Table 2 at 96-second time resolution. This represented a single subcom sample of the single-detector rates, and 96-second averages of the LAZ3* and TAN rates. These would be redundant with the Neptune 6-second data described in Section 2.2, and inferior for LAZ3* and TAN with each datapoint being an average over 16 of the 6-second datapoints. However, these data fill in some of the gaps during 1989 day 237, and add four hours at the start of the encounter from day 236, so we are including them in our PDS/PPI submission, as file "rates_96sec_n.csv". A comparison of the LAZ3* data from the two datasets is shown in Figure 2. The CSV file contains one header line giving column titles, followed by rows each giving data for a single 96-second volume.

Figure 2

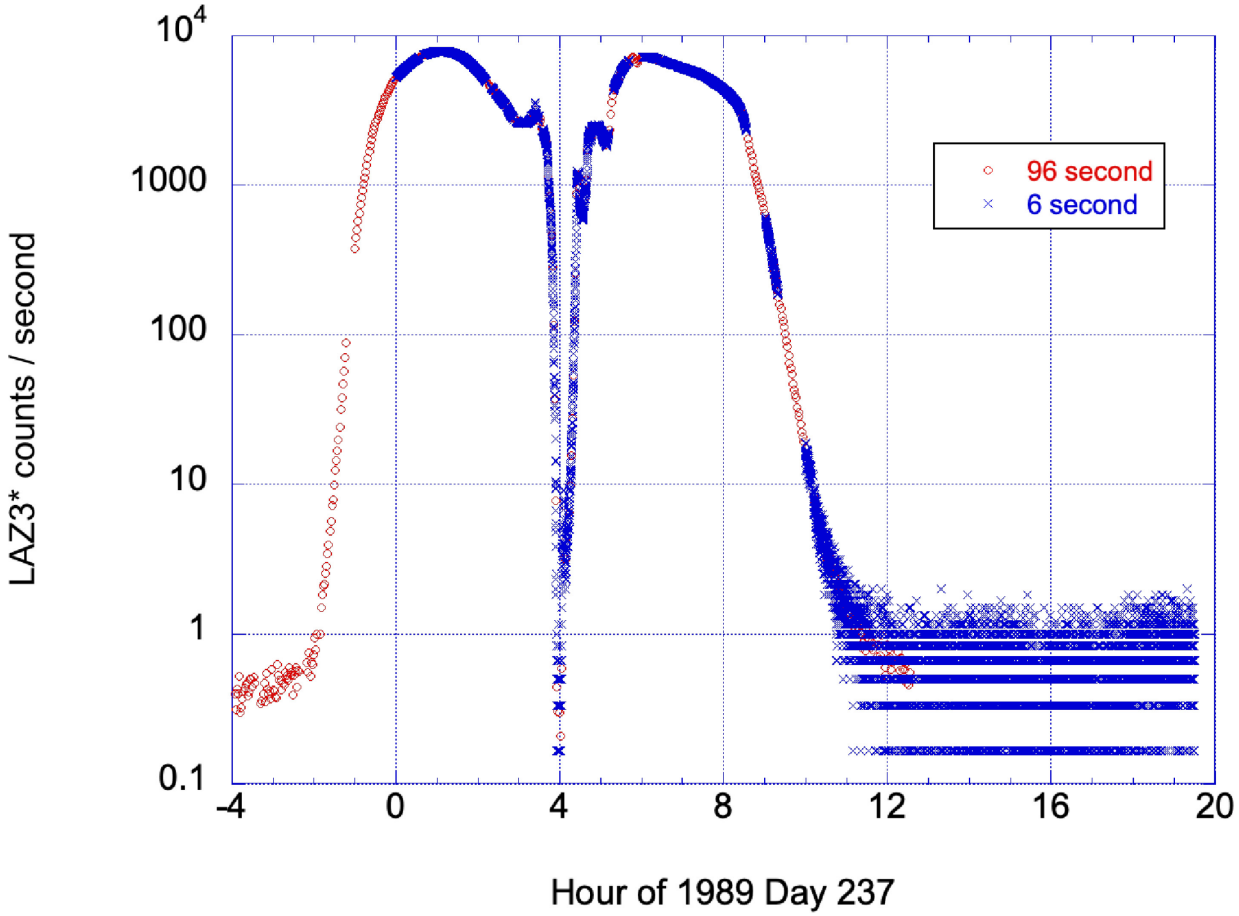


Figure 2: Comparison of 6-second (GSFC) and 96-second (PI's thesis) LAZ3 countrates.*

The columns in the CSV file are (1) the volume number; (2) the time of the middle of the volume as decimal hours of 1989 day 237 (including negative numbers for the last four hours of day 236); and (3-9) counts per second for LAZ3* from LET A, TAN, D1L, and D2L from TET, and LA1, LC1, and LD1 from the respective LETs. Fill value is -1.

2.3.1. Timing of the Neptune Data

The timestamp for each row of the 96-second data is for the midpoint of the 96second time period. The countrates in that file for LAZ3* and TAN will be averages of (up to) 16 samples during this period; however, the single-detector countrates will be from the 6second accumulation time having the appropriate subcom state within that period, so a user can adjust that to match the timestamps in "rates_6sec_n.csv" if desired. A minor point to note is that the timestamps in both the 96-second rate data and the proton flux data are aligned to the start of day 237, with volume 4157100 beginning at second 0; the 6second rate data are

one second off, with that volume's subcom 0 start occurring on the last second of day 236. One second is not a large fraction of 96 seconds or 192 seconds, but we mention it for completeness.

3. References

Cooper, J. F. and E. C. Stone, "Electron Signatures of Satellite Sweeping in the Magnetosphere of Uranus," *J. Geophys. Res*. **96** (A5), 7803-7821 (1991), DOI: 10.1029/90JA02629

Garrard, T., "MJS CRS Science Requirements Document," Space Radiation Laboratory Technical Report 76-1 (revised 1978), available online at https://voyager.gsfc.nasa.gov/Library/SRL_Technical_Report_76-1_SRD.pdf

Garrett, H., and R. Evans, "The JPL Neptune Radiation Model (NMOD)," JPL Publication 17-2 (2017), online at https://ntrs.nasa.gov/search.jsp?R=20170006886

Looper, M. D., "Energetic Protons in the Magnetosphere of Neptune," PhD dissertation in Physics, advised by Prof. E. C. Stone, Department of Physics, Mathematics, and Astronomy, California Institute of Technology (1993), DOI: 10.7907/QEPK-4523

Selesnick, R. S., and E. C. Stone, "Energetic Electrons at Uranus: Bimodal Dieusion in a Satellite Limited Radiation Belt," *J. Geophys. Res*. **96** (A4), 5651-5665 (1991), DOI: 10.1029/90JA02696

Stone, E. C., et al., "Energetic Charged Particles in the Magnetosphere of Neptune," *Science* **246**, 1489-1494 (1989), DOI: 10.1126/science.246.4936.1489

Appendix A. History of This Augmentation Project and Provenance of Data

This project originated when H. Garrett contacted the PI, M. Looper, for permission to include several plots from the latter's PhD thesis (Looper, 1993) in the Neptune radiation model (NMOD) that he was assembling (Garrett & Evans, 2017). These included proton fluxes from LET C and LET D, as discussed in Section 2.1, for five energy channels spanning 1.9 to 5.0 MeV. M. Looper remembered that he still had paper plots for energy channels up to 7.8 MeV in his files, and while searching for those he found several other plots with countrates and other data beyond what was in the thesis and published journal articles. It was decided that, since these were the only surviving copies of this data, it should be digitized from the plots and submitted to PDS/PPI so that it could be of use to others studying the outer planets. A Step-1 proposal was prepared for a NASA ROSES PDART (Planetary Data Archiving, Restoration, and Tools) project to do this.

Then, while M. Looper and J. Mafi of UCLA and PDS/PPI were preparing the Step-2 proposal, the former got in contact with his long-ago Voyager colleague A. Cummings at the Caltech Space Radiation Laboratory, where the thesis was written. He provided additional plots from his notebooks (some of which are reproduced with permission in Appendix B), and suggested that we contact N. Lal at GSFC. When we did this, we discovered that he still had access to the Voyager encyclopedia files not only from the Neptune encounter but also from Uranus! He agreed to provide us in digital form with much of the data that we had been planning to digitize from paper plots, which meant that we could provide it to PDS/PPI in much greater fidelity and with full time resolution, and he joined the proposal as a collaborator.

After the proposal was selected, we had another serendipitous discovery. M. Looper stumbled across thirty-year-old backup tapes from his thesis research in a box at his home, and S. Joy of UCLA and PDS/PPI was able to find a vendor to read them! It turned out that these contained the data that went into all of the proton flux plots, as well as additional rate information as discussed in Section 2.3. This meant that we could completely dispense with the digitizing of paper plots. In addition to time-series graphs like that in Figure 3, our collection included plots of spectra vs. energy at different times, and of flux vs. L, as well as some plots with zero-flux points (upper limits only) omitted so that nonzero points stood out more clearly; thus we had expected to be able to separate the points and error bars that lay on top of each other in, e.g., Figure 3. *HET 1 high-gain coincidence rates at Neptune, as submitted.*, but it would have been an arduous and error-prone process. The data files discussed in Sections 2.1 for proton flux and Section 2.3 for miscellaneous rates were quickly assembled from the recovered files. Thus this data is taken directly from files created during the period of the Neptune encounter, as described by Looper (1993), and we have confirmed that it matches what went into the thesis, other published journal articles, and NMOD.

After so much good luck, however, we were greatly saddened when N. Lal, a longtime colleague and friend who had been with Voyager from the start, passed away suddenly about a year into this project. Apart from our personal loss, this also made it uncertain if we would be able to obtain the data that he had been preparing to send us, as none of it had been sent yet. The Voyager team, of course, had to scramble to find successors for all the roles he had played in the ongoing Voyager Interstellar Mission, and those people had a lot to do with their present tasks as well as the ones they took over from their late colleague. B. Heikkila took over his work at GSFC, and despite having no formal obligations to this proposal at all, he generously agreed to look at what N. Lal had been preparing for us.

This proved difficult, as anyone who has dug through another's code can attest. He found some files from Neptune that appeared to be nearly ready for delivery, and was able to get N. Lal's old programs running so as to attempt to strip more rates and/or more time periods. However, the contents of the code and its input binary files were not documented, and the control files that directed the stripping program were likewise not documented, so the ability to fill in data gaps beyond what had already been done was limited (e.g., as noted in

Section 1.2, we never were able to obtain data from 1989 day 236 at the start of the Neptune flyby). Moreover, the output files were variable as to their clarity; modes and subcom states as discussed in Section 1.2.1 were not identified, and in some files fill values were -1 but in others they were 0, meaning that we had to sort out which zeroes were real and which were fill in the latter files. Some of the rates did not appear to match the labels assigned to them; in particular, there was confusion between the TLO and THI rates for TET, and the high- and low-gain counterpart rates for HET 1 (e.g., A2L and A2H) were usually but not always listed in each others' columns in the files.

These files were clearly works in progress, which is why N. Lal had not sent them to us yet. However, as noted in Section 1.2.1, we found a concise summary of the subcom and mode organization of the rates in his source code (confirmed with the CRS SRD, Garrard 1978), and we were able to correlate this with the tabulated rates to assemble a consistent and coherent sequence of modes and subcom states. The LET coincidence rate file included LCX2, LCX3, LDX2, and LDX3 sorted from LCZ3* and LDZ3*, so we could use their cycling to confirm the H2/L3 mode sequence, and the TET and LET single-detector rates allowed us to line up the subcom states. We then used this information to sort out the HET1 singles rates; this is how we determined that the high- and low-gain counterpart rates were usually switched (that is, a valid high-gain rate would be found in the correct subcom state and in H2 mode but in the low-gain rate's column while a fill value would be found in the high-gain rate's column at that time, and vice versa). With this information we were able to combine the data in the two columns to fill out both; unfortunately, A1, B1, and C1 were only present in high gain, so as can be seen from the plots in Appendix B, data for the rates IA1H, IB1H, and 1C1H are very sparse, since only occasionally did a non-fill value appear during H2 mode in the stripped data.

B. Heikkila was also able to locate N. Lal's Uranus encyclopedia file, and to get his rate-stripping code to run, so he was able to supply us with the same set of rates for the Uranus flyby. We were able to apply the same analysis to assign a mode and subcom state to each time-stamped entry and assemble the data into the CSV file that is part of our PDS/PPI submission. The data files delivered from GSFC consisted of separate ASCII files for each of HET 1 single-detector rates, HET 1 coincidence rates, HET 2 singles, HET 2 coincidence, LET singles, LET coincidence, and TET combined. We were not able to identify with confidence the rates in the coincidence files for either HET 1 or HET 2; some columns consisted entirely of fill values, and there were extra columns that we could not associate with a rate using the control files (there were no column headers in the data files themselves). However, among the files that B. Heikkila found were some Neptune test files with earlier creation dates than those that we used to create most of our PDS/PPI submission, and among those was "het1_listing5.txt", which contained the five HET 1 coincidence rates highlighted in yellow in Table 2. These *were* fairly complete (within day 237), unlike the high-gain HET 1 data in the later files, and (1) IAS looked commensurate with a coincidence of A1H and A2H as in the table in Figure 1; (2) IBSp and IBSe matched the subcom pattern listed in Table 2; and (3) IPENH was similar to but slightly

higher than IPGH, which is consistent with the latter being the same as the former but with a guard anticoincidence, again as in Figure 1. See Figure 4 below for a plot of four of these rates.

To summarize the provenance of the data, then, the proton fluxes at Neptune were taken from files recovered from M. Looper's backup tapes and confirmed against paper plots. The 96-second rates at Neptune were also taken from those tapes, and checked against the 6-second rates. The 6-second rates were assembled from files created either by N. Lal or by B. Heikkila using his code and input files. Mode and subcom state for each 6-second time interval at each planet's flyby were identified using TET and LET data, HET 2 data were taken from the files and confirmed against the subcom state (HET 2 was always in low-gain mode during both encounters), and HET 1 singles were assembled from mixed (nominal) high- and low-gain rate columns in the files and assigned to the appropriate gain state based on the LET determination of H2/L3 mode state. For Neptune, we found another file in Nand Lal's test data that contained five high-gain HET 1 coincidence rates, which we confirmed against mode and subcom state and other characteristics and added to our submission.

Clearly more could be added to the data from both flybys, but only with significant additional effort to understand N. Lal's code and data files. Besides filling in missing time periods and sorting out the mostly-missing high-gain HET 1 data as described above, N. Lal had planned to send us the pulse-height data to preserve at PDS/PPI, and he never had the chance to do so. We had proposed to use the pulse heights from detector LA1 to extend the proton spectra to energies lower than the 1.9 MeV lower limit of the LET C and LET D doubles, and potentially someone could use, e.g., the analysis methods of Looper (1993) to derive proton fluxes at Uranus or of Selesnick and Stone (1991) to derive electron fluxes at both planets. We hope that our recovery of this data from the Uranus and Neptune flybys will motivate others to pursue additional data in N. Lal's files; and, of course, we hope that our story of data discovered on thirty-year-old plots and backup tapes, and the difficulty of recovering additional data following the retirement or passing of its custodians, will motivate other investigators to preserve their own data for future users while they can.

Appendix B. Plots of Six-Second Neptune Countrates

As mentioned above, the files we received from GSFC did not have column headers, so we had to identify countrates based on our understanding of N. Lal's control files and check them against the mode and subcom states appropriate for each rate per Table 2. We also had several plots of rates from the Neptune flyby, which we had borrowed from A. Cummings, and we used those to confirm our identification of those rates, which gave us confidence to make the same identifications in the Uranus data for which we did not have plots. We reproduce scans of his plots here, with permission, alongside plots of the corresponding rates in our PDS/PPI submission with the same time and rate axis ranges for comparison. In Figure 3 below, we show four of the five HET 1 high-gain coincidence rates (IBSp was sensitive to high-energy

protons, and never rose above a few counts per six seconds) that composed the extra file that we used to add these to the Neptune 6-second rates, as discussed in Appendix A.

Figure 3

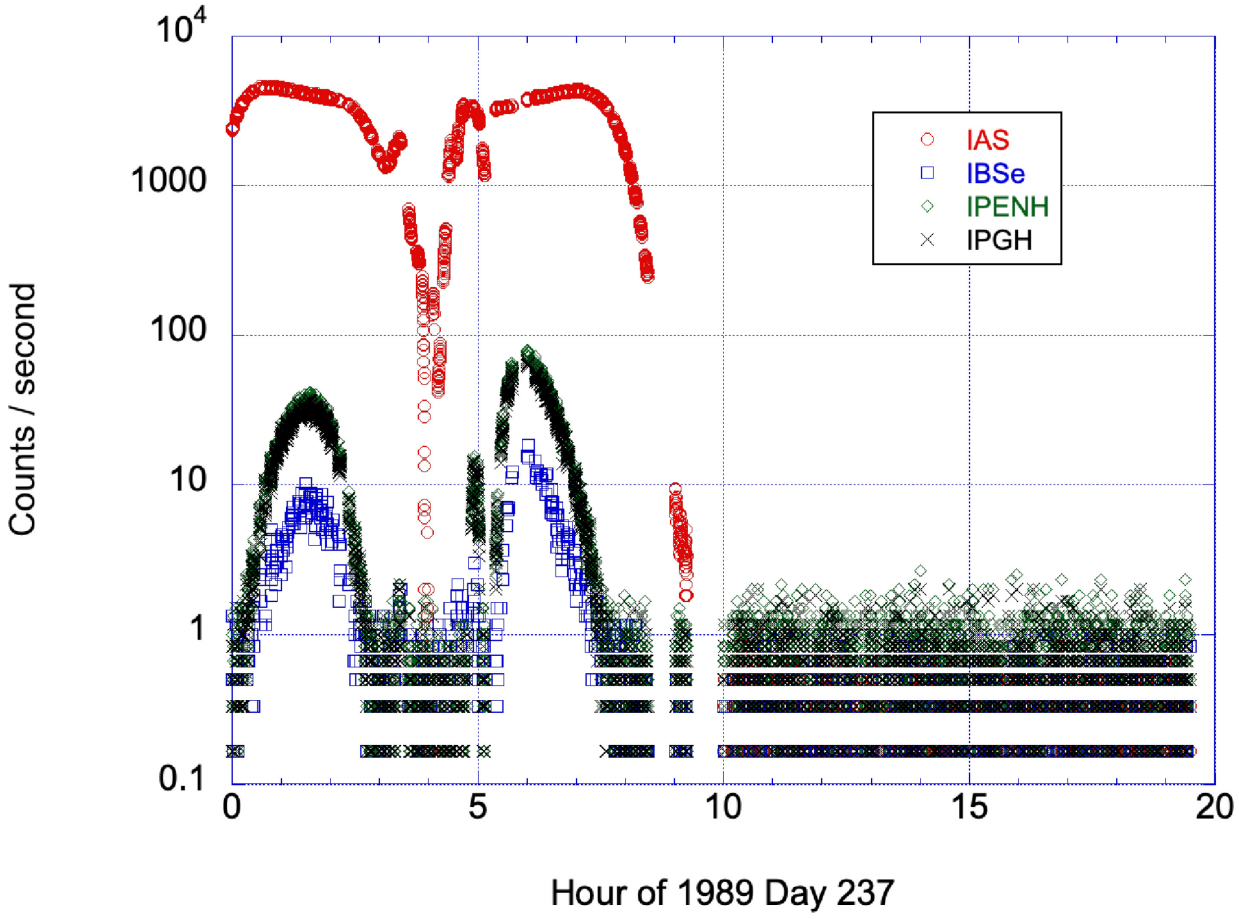
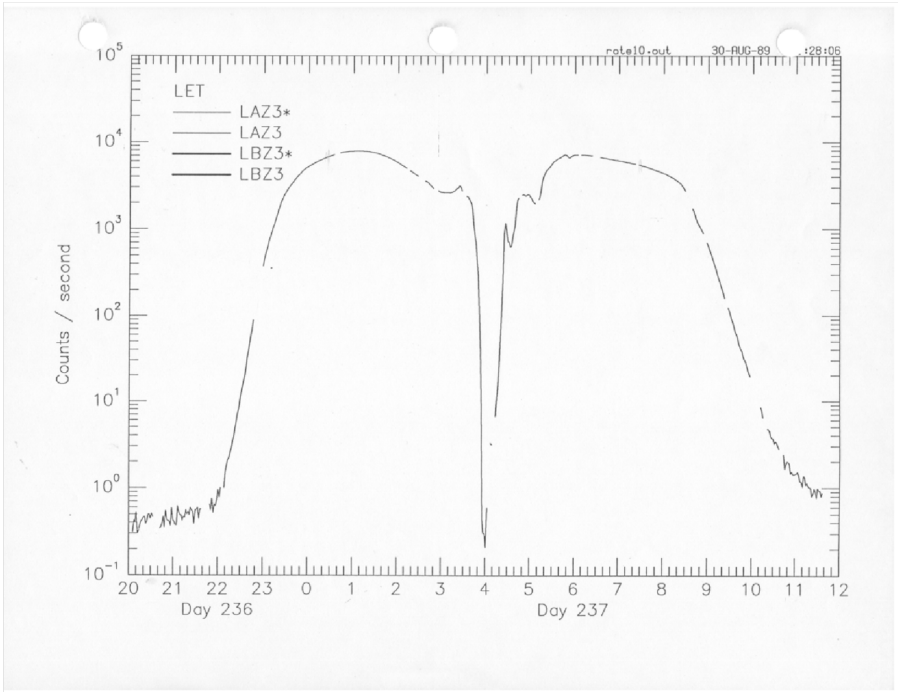


Figure 3. HET 1 high-gain coincidence rates at Neptune, as submitted.

Figure 4



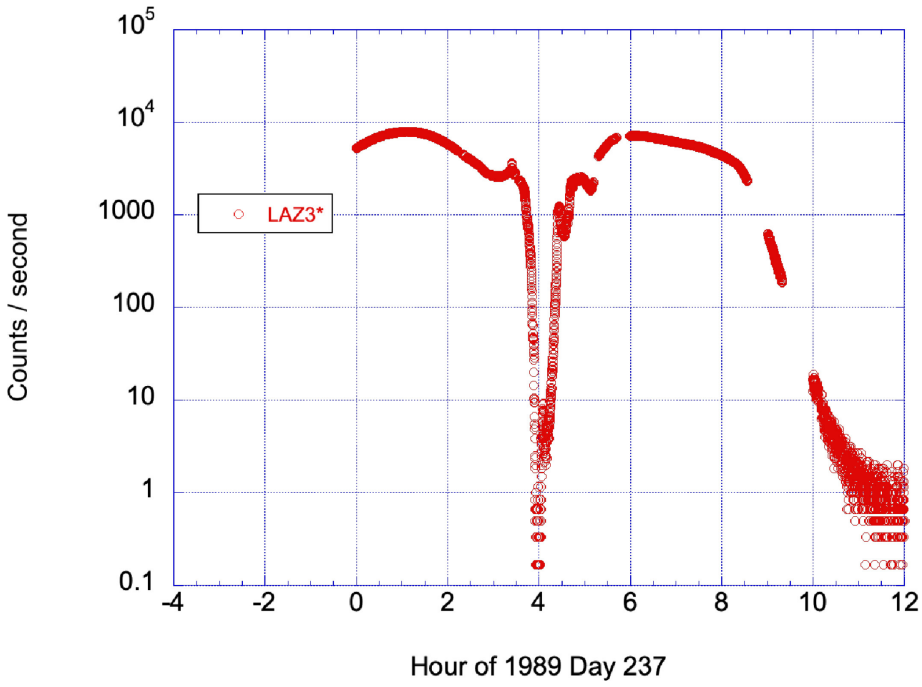


Figure 4. LET LAZ3 at Neptune, scanned plot and data as submitted.*

Figure 5

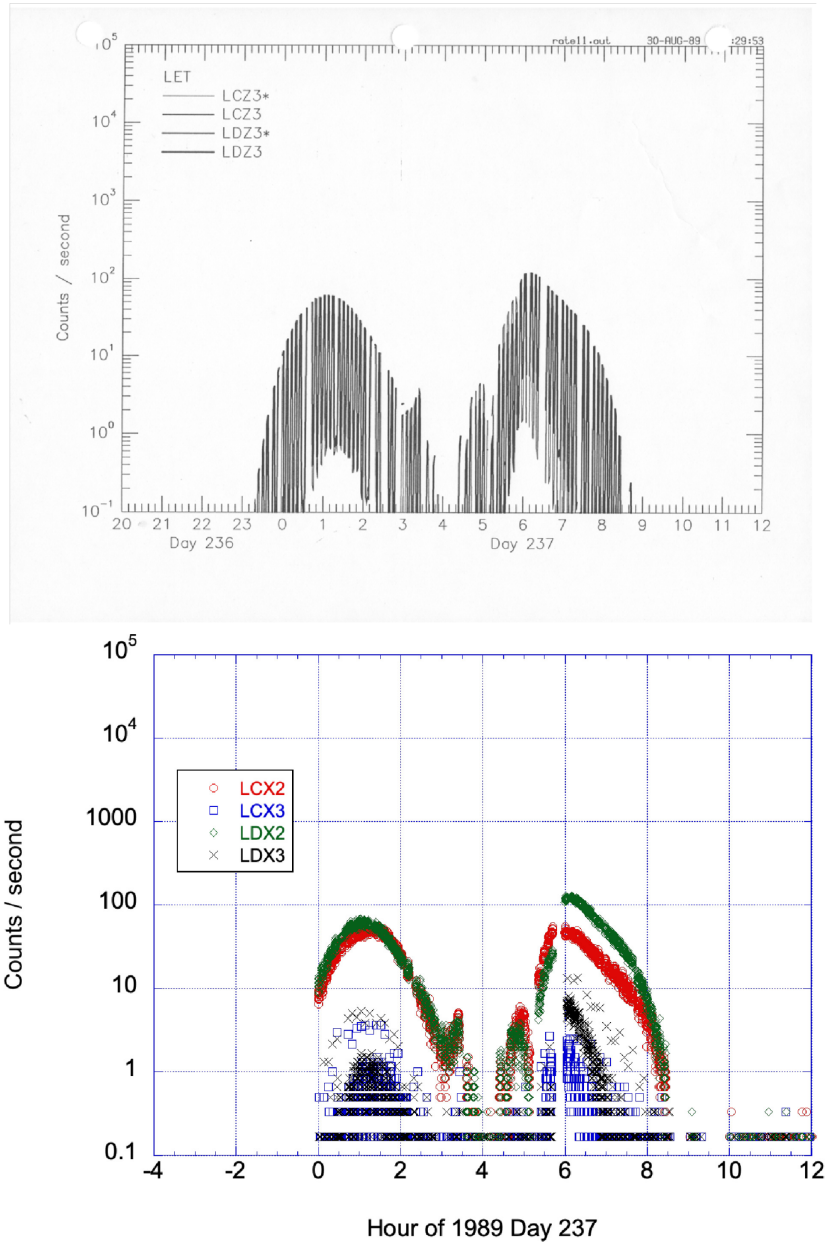


Figure 5. LET C and D coincidence rates at Neptune, scanned plot and data as submitted.

Figure 6

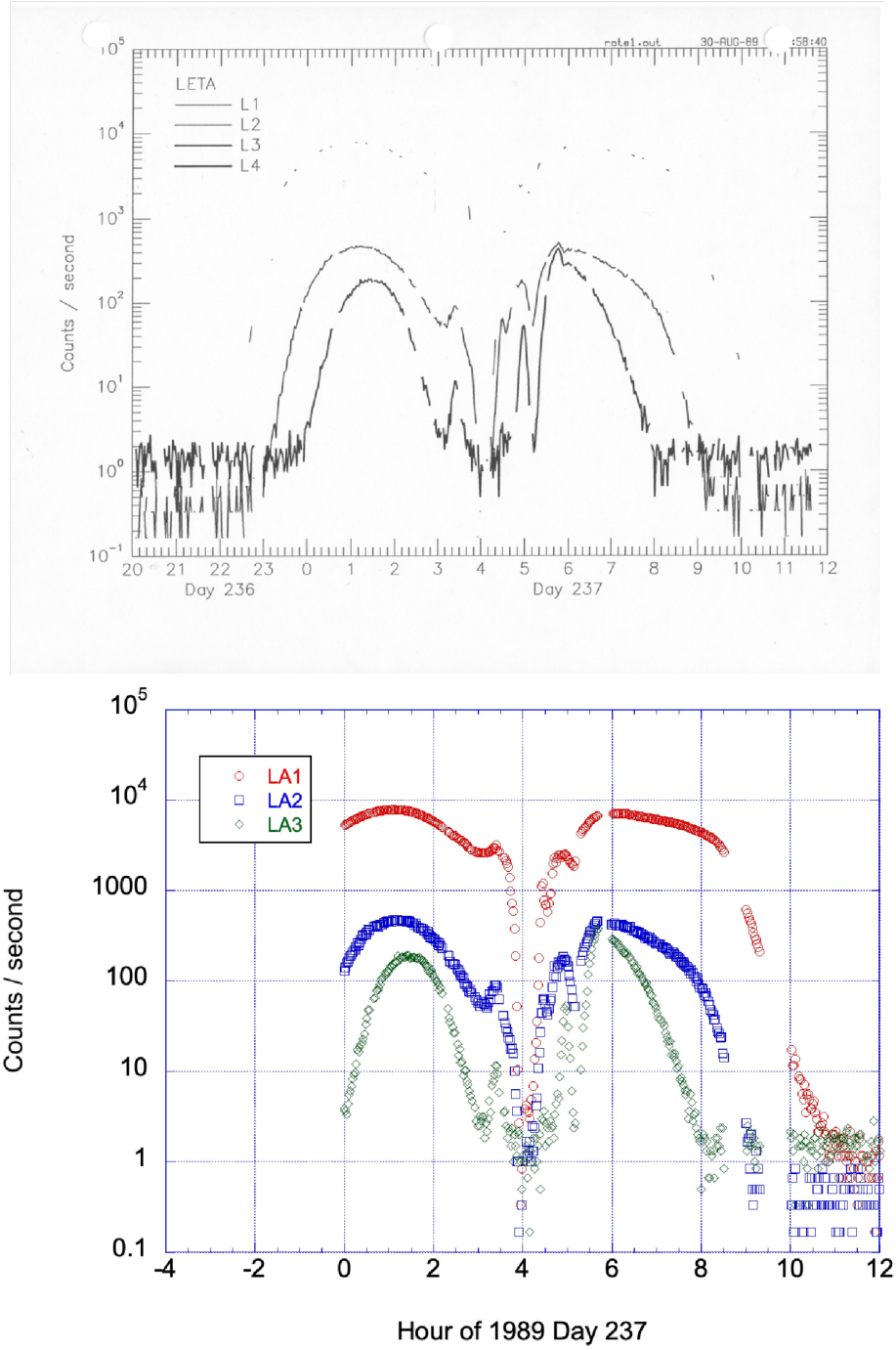
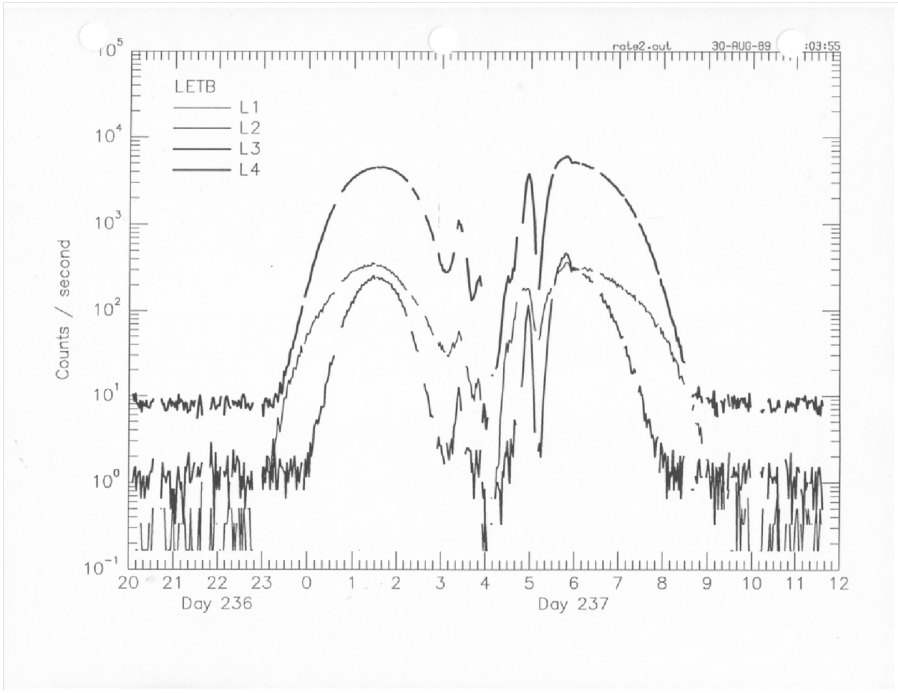


Figure 6. LETA singles rates at Neptune, planned plot and data as submitted.

Figure 7



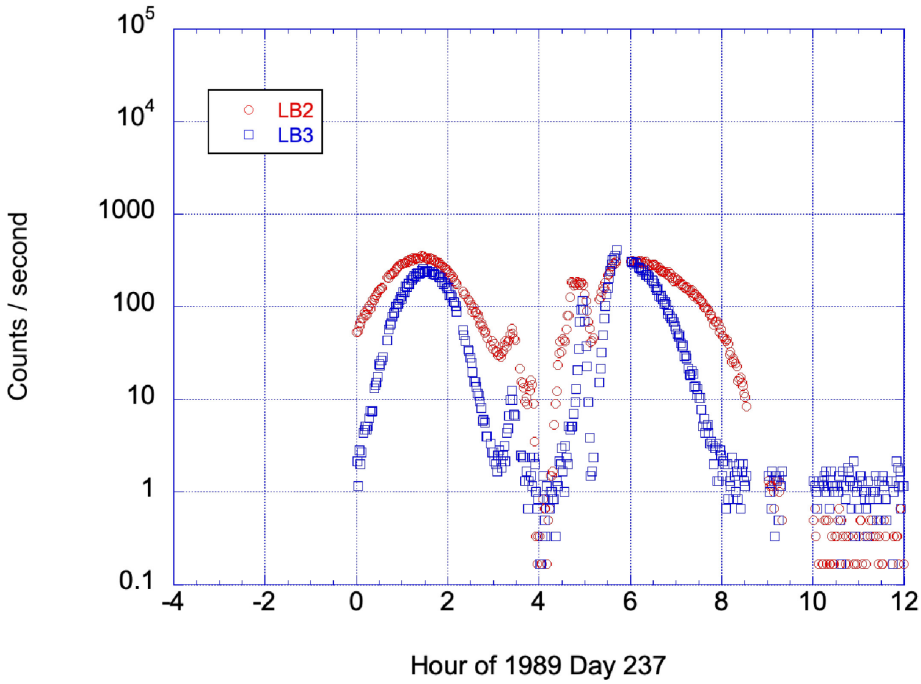


Figure 7. LET singles rates at Neptune, scanned plot and data submitted.

Figure 8

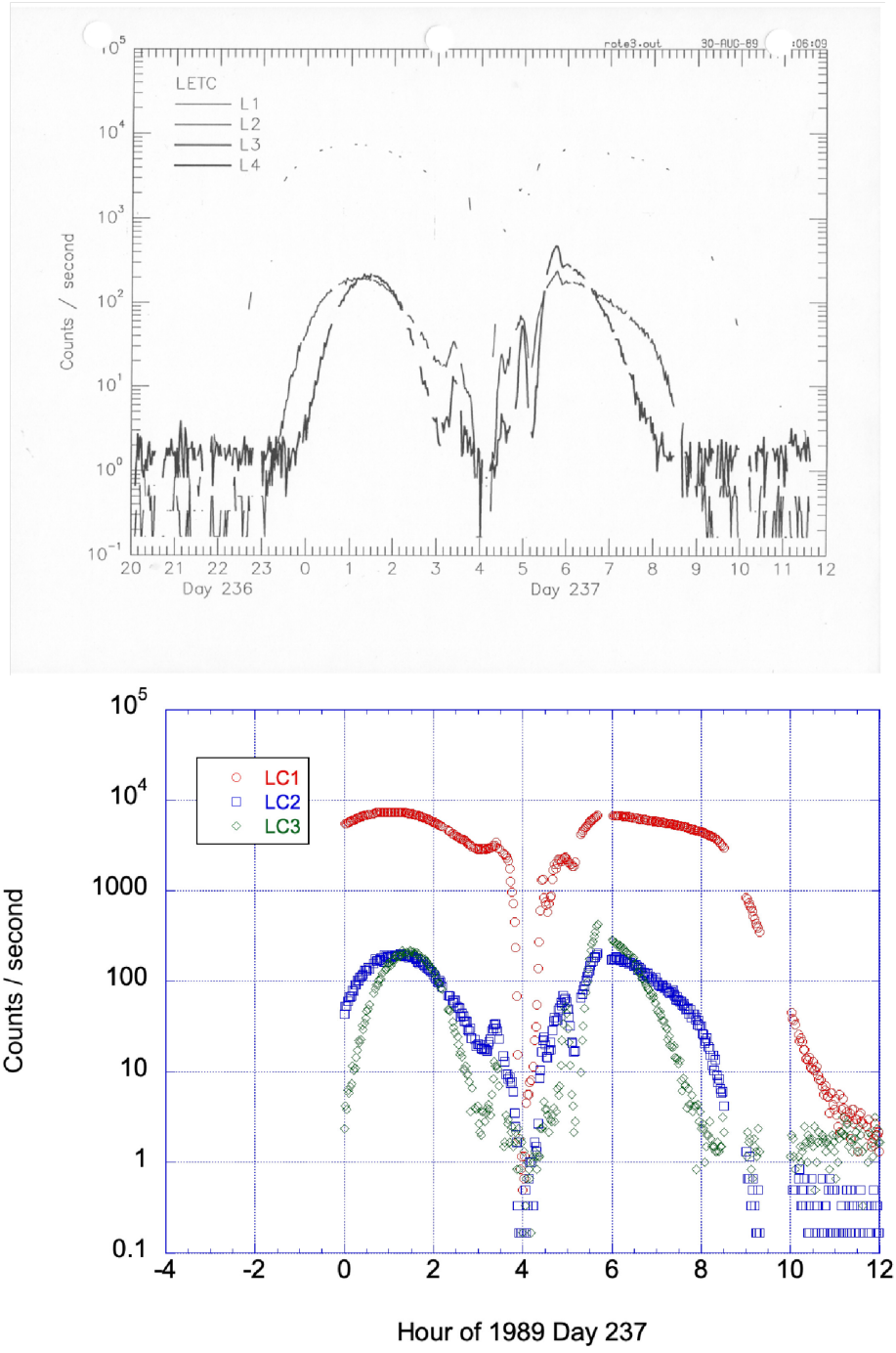


Figure 8. LET C singles rates at Neptune, scanned plot and data submitted.

Figure 9

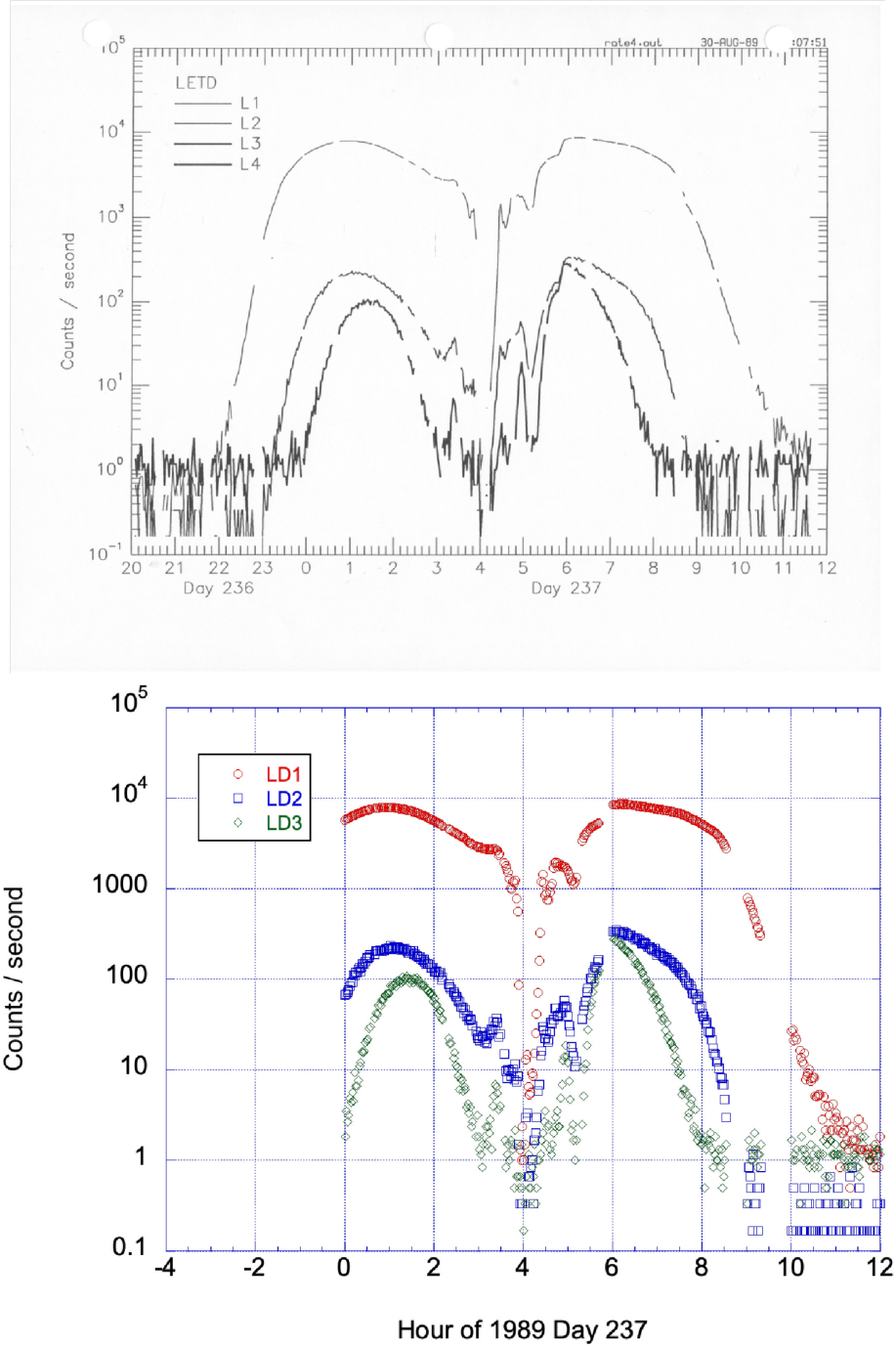


Figure 9. LET D singles rates at Neptune, scanned plot and data submitted.

Figure 10

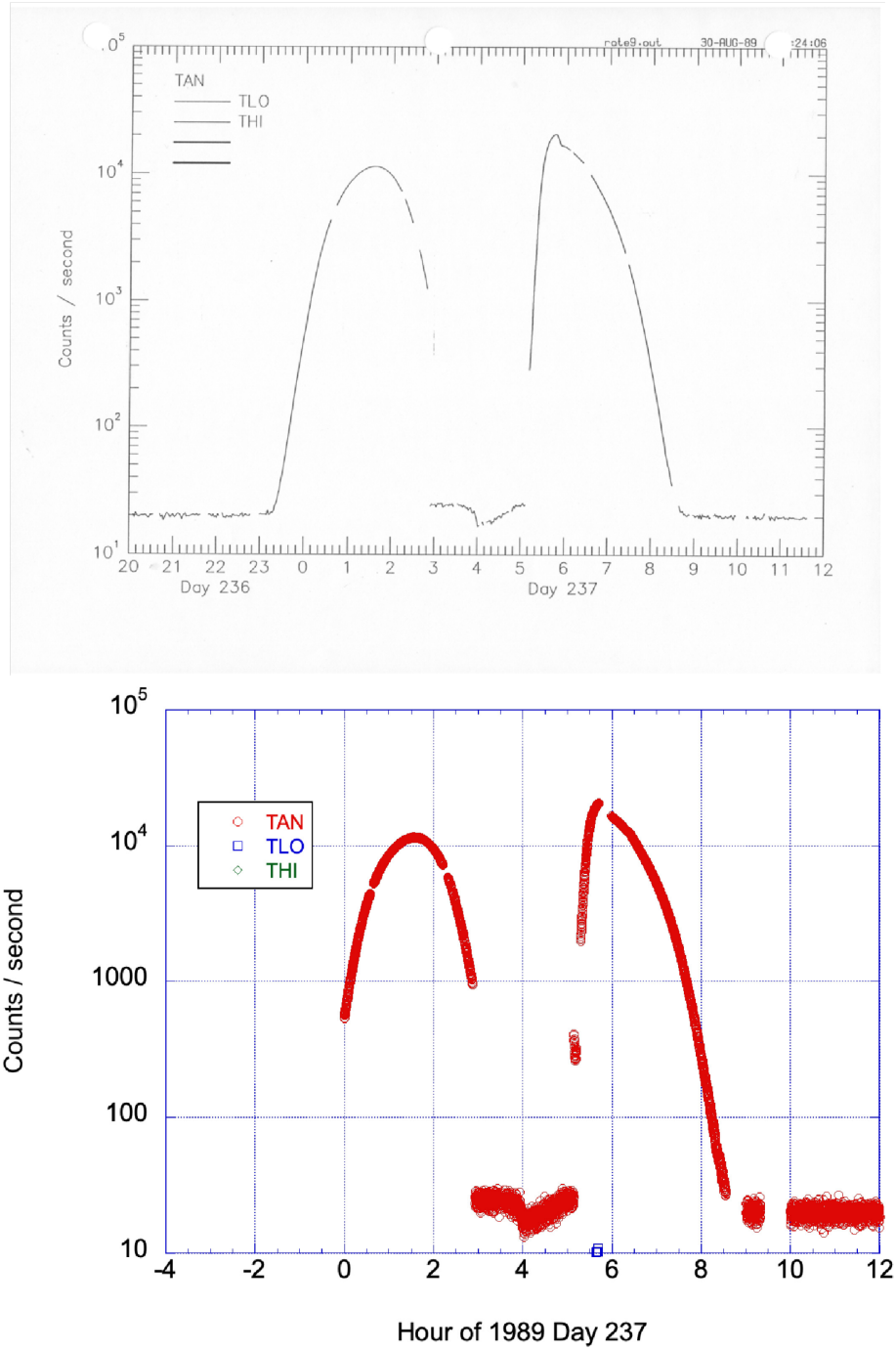


Figure 10. TET coincidence rates at Neptune, scanned plot and data as submitted.

Figure 11

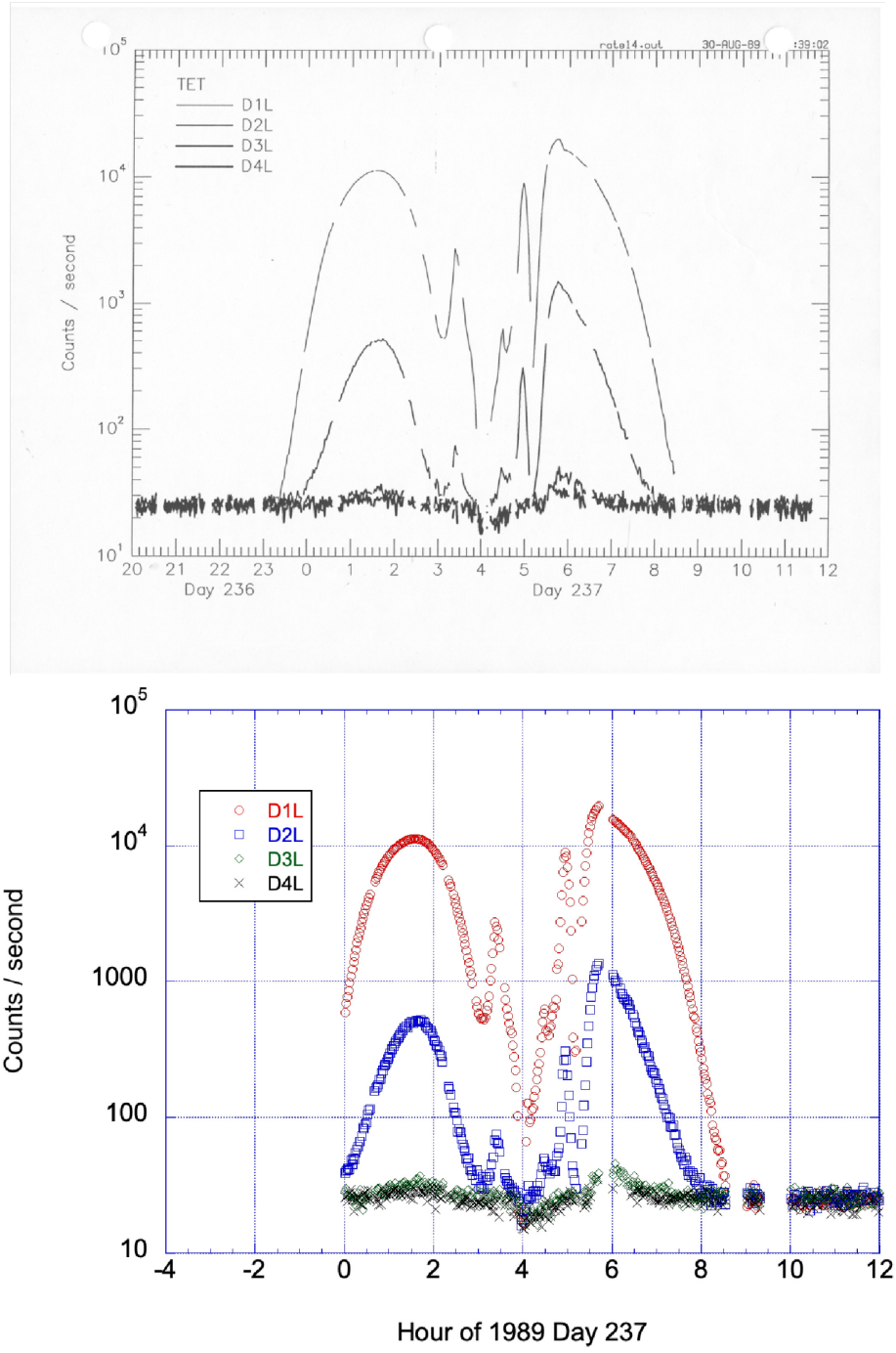
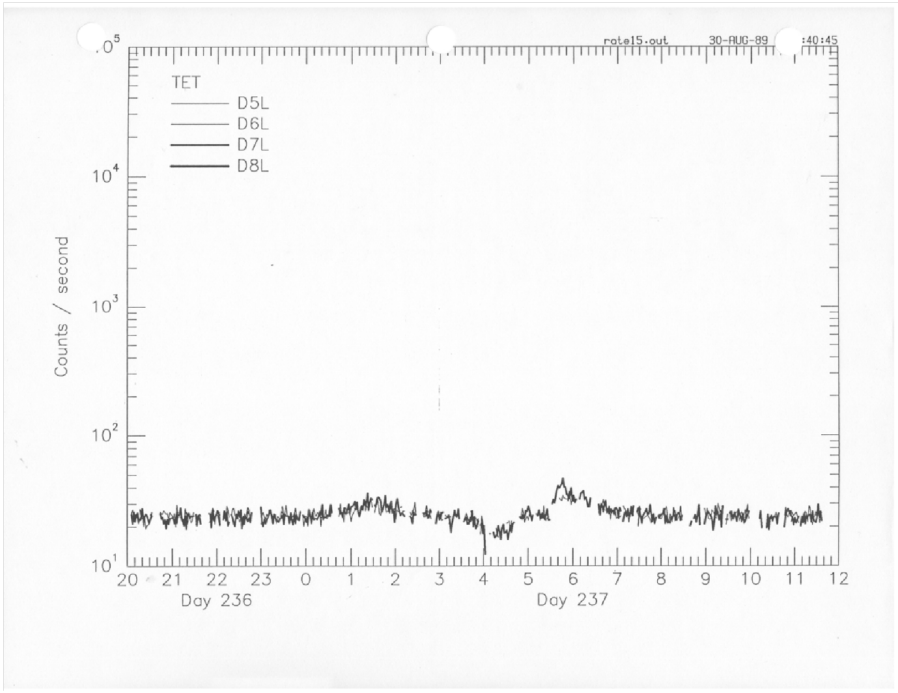


Figure 11. TET singles rates at Neptune, scanned plot and data as submitted.

Figure 12



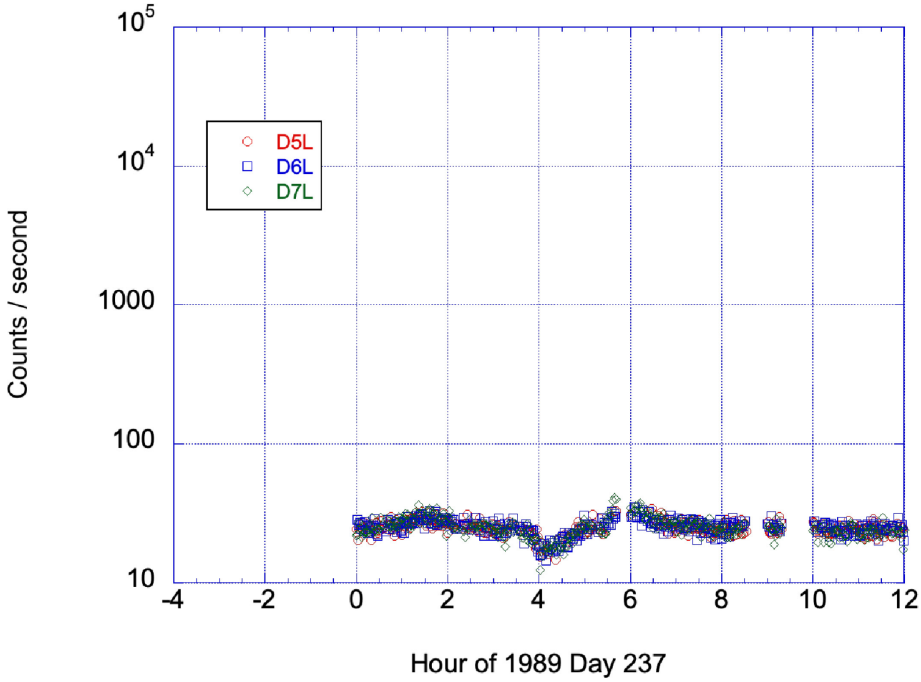
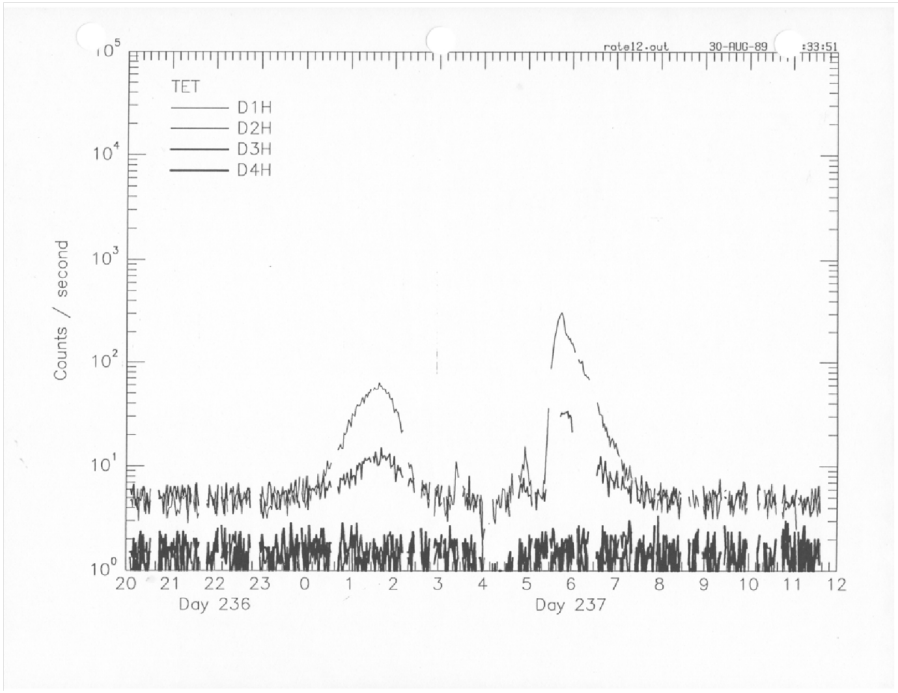


Figure 12. TET singles rates at Neptune, scanned plot and data as submitted.

Figure 13



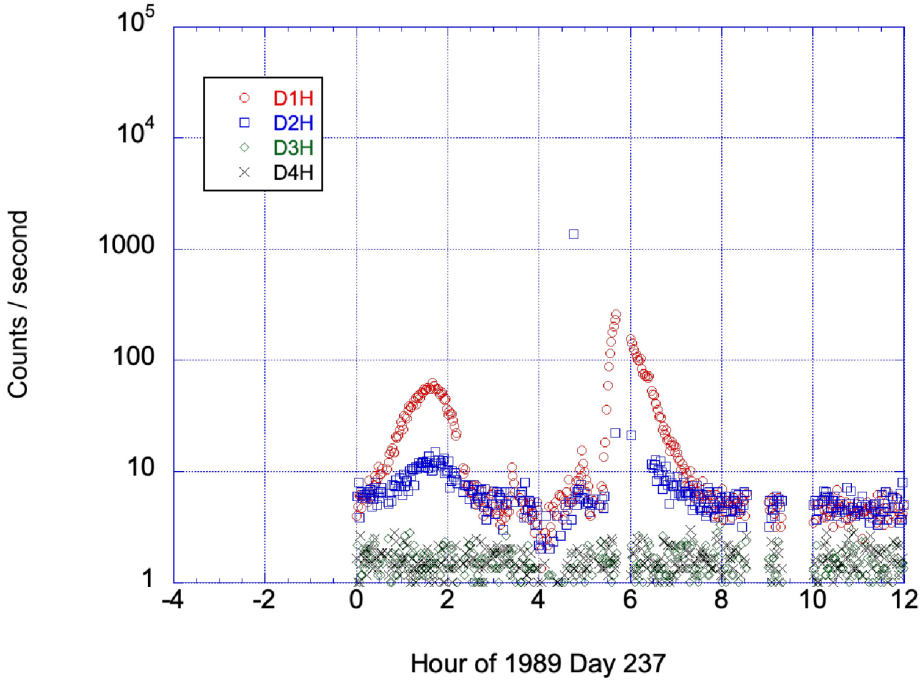


Figure 13. TET singles rates at Neptune, scanned plot and data as submitted.

Figure 14

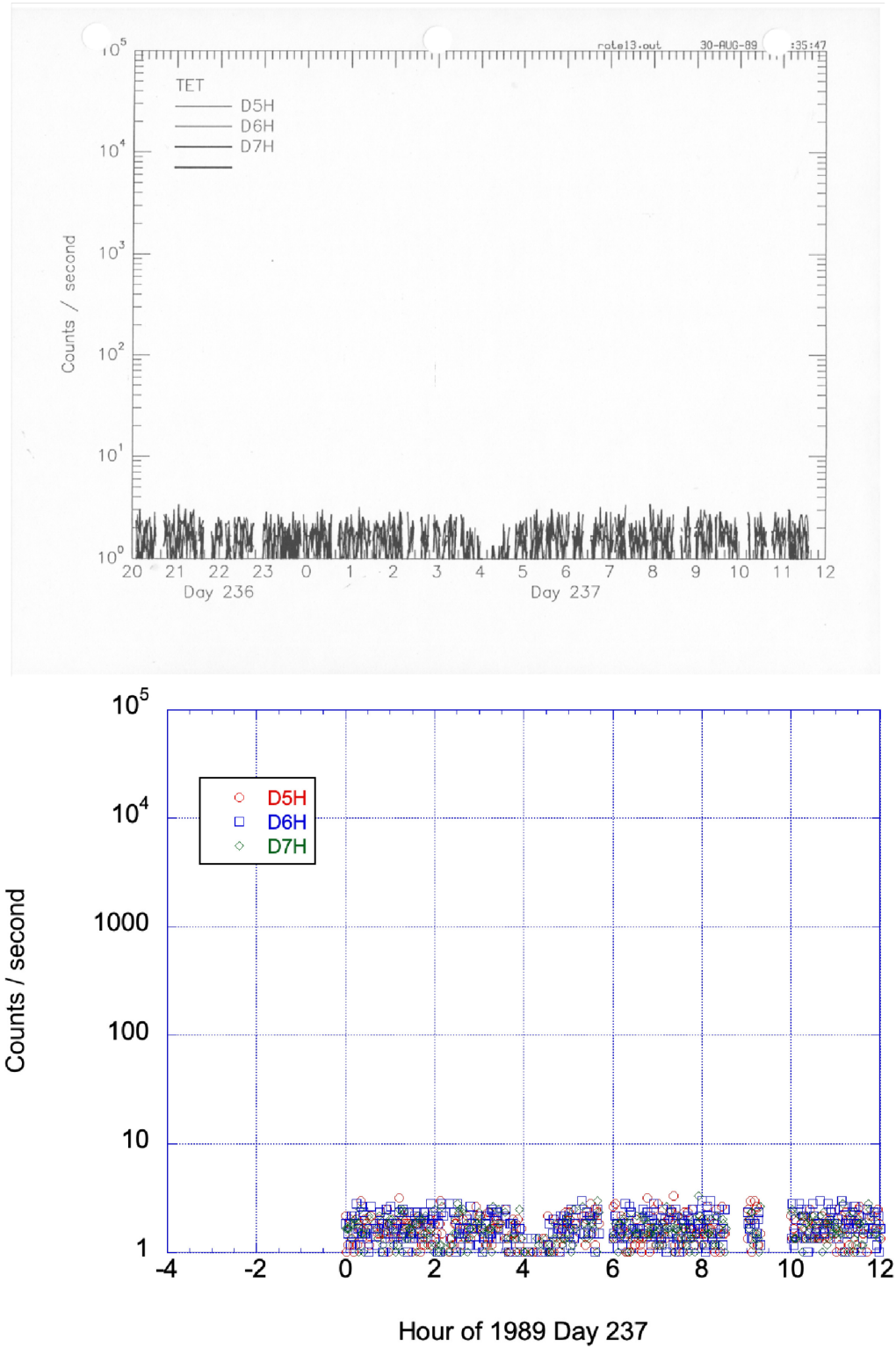
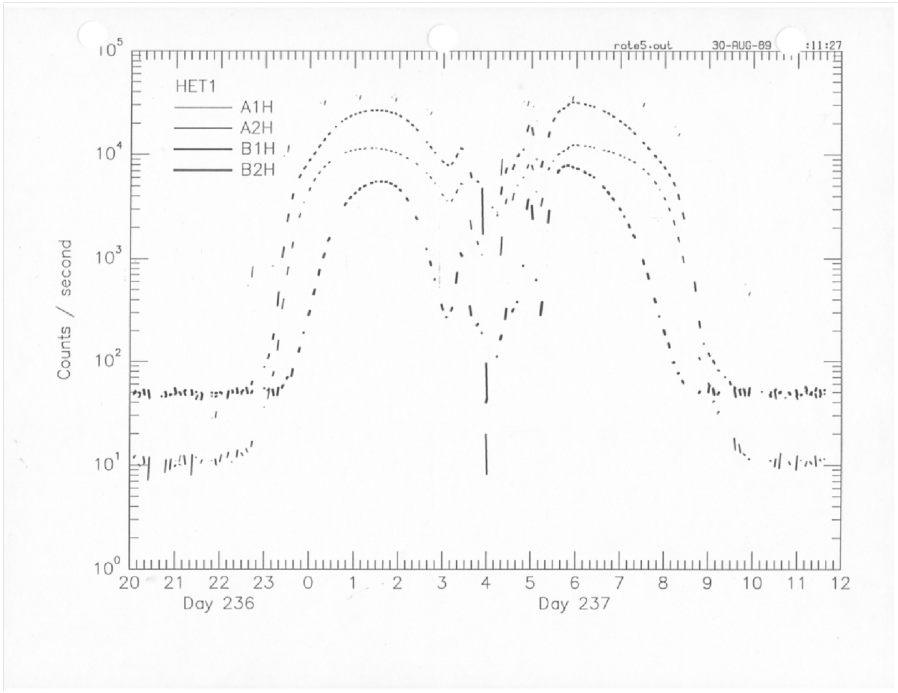


Figure 14. TET singles rates at Neptune, scanned plot and data as submitted.

Figure 15



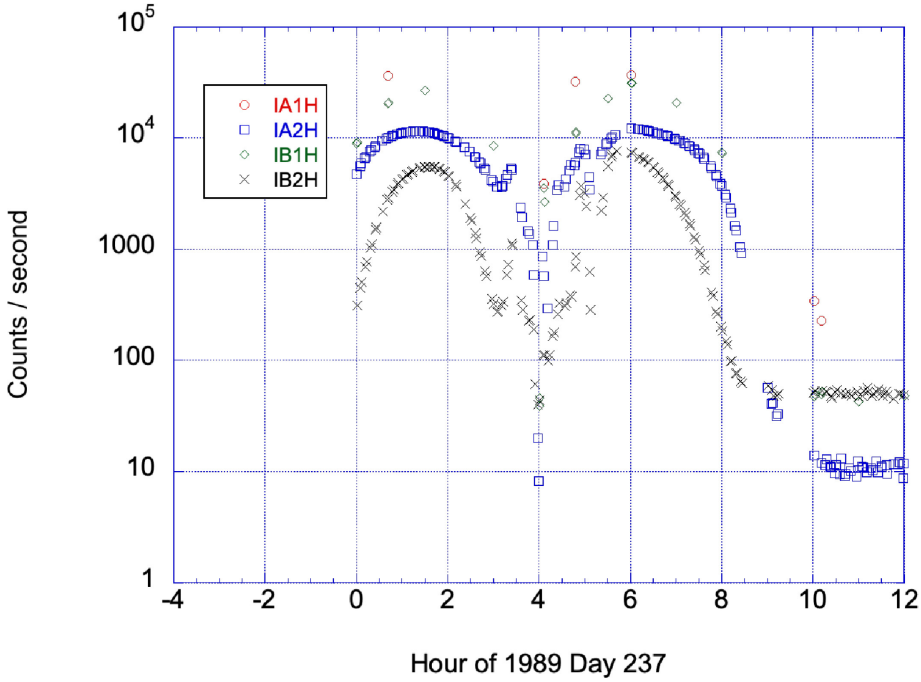
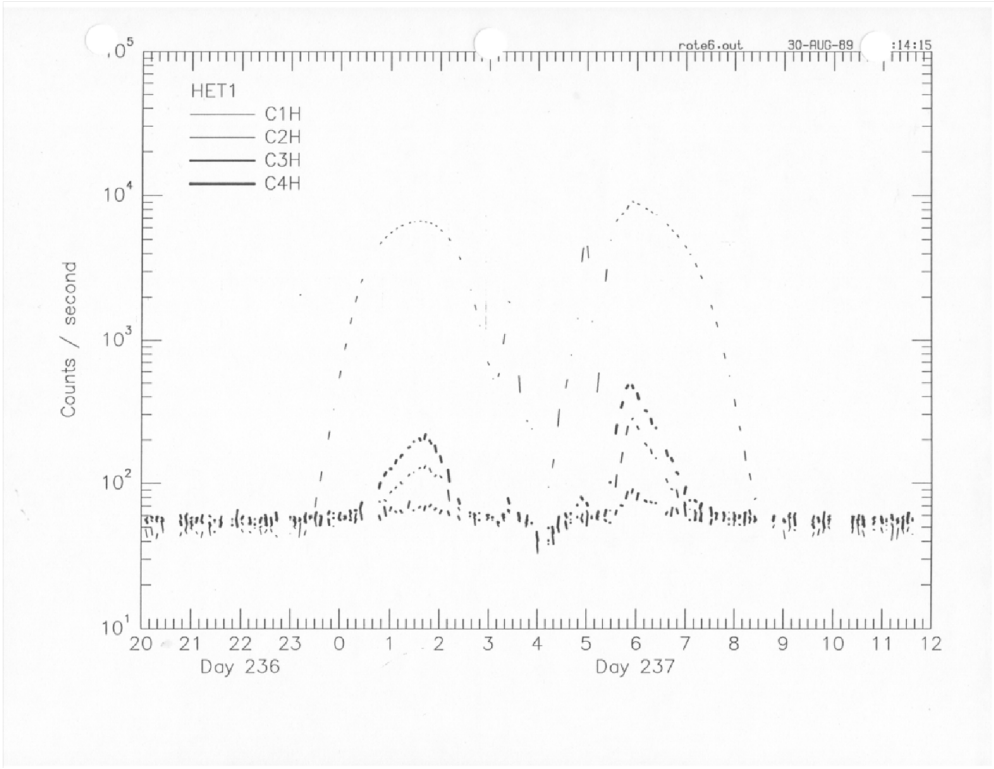


Figure 15. HET 1 singles rates at Neptune, scanned plot and data as submitted.

Figure 16



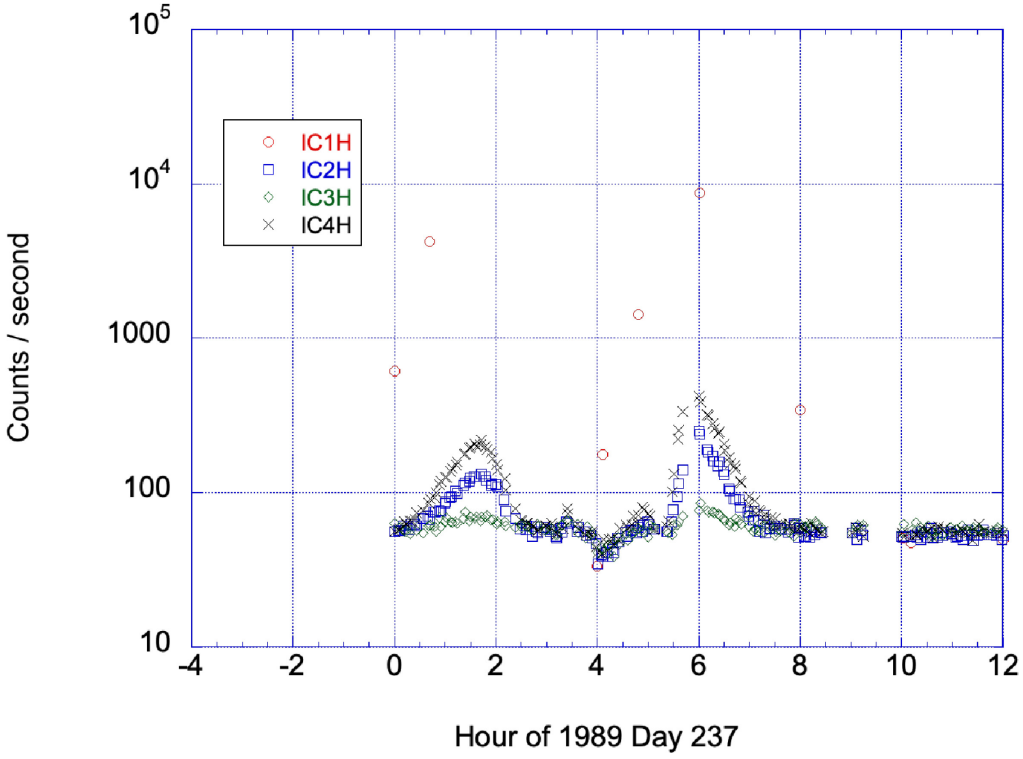


Figure 16. HET 1 singles rates at Neptune, scanned plot and data as submitted.

Figure 17

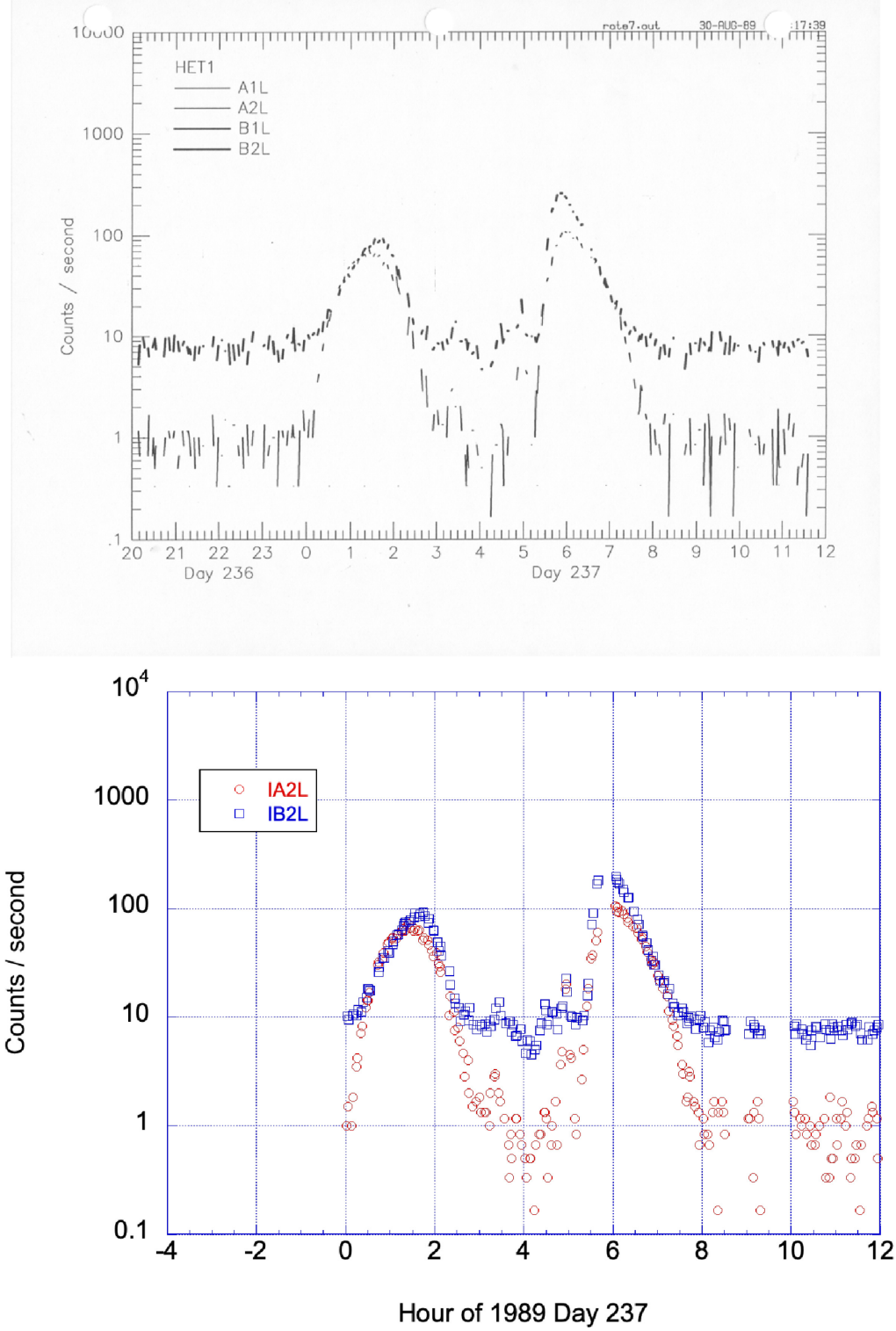


Figure 17. HET 1 singles rates at Neptune, scanned plot and data as submitted.

Figure 18

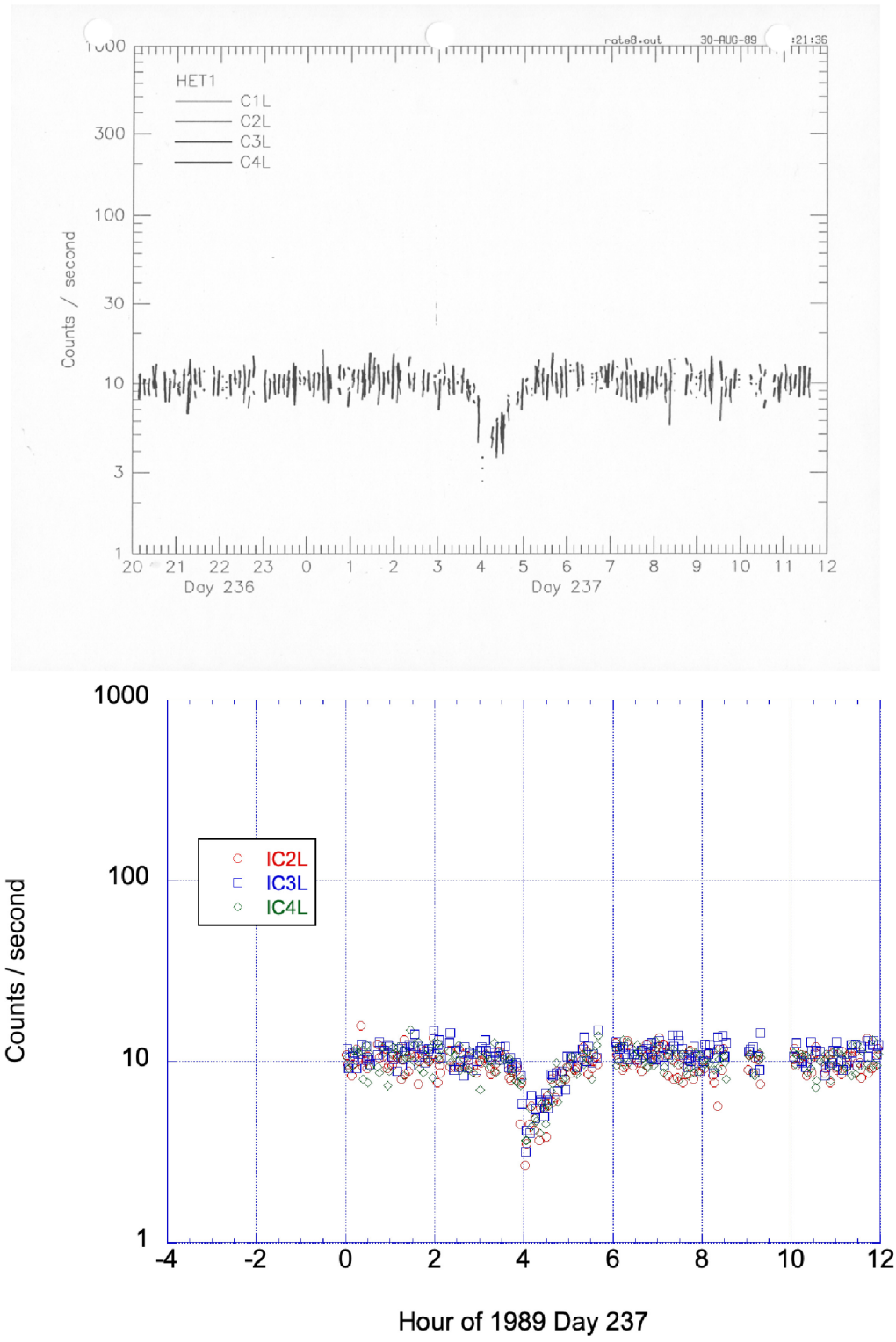
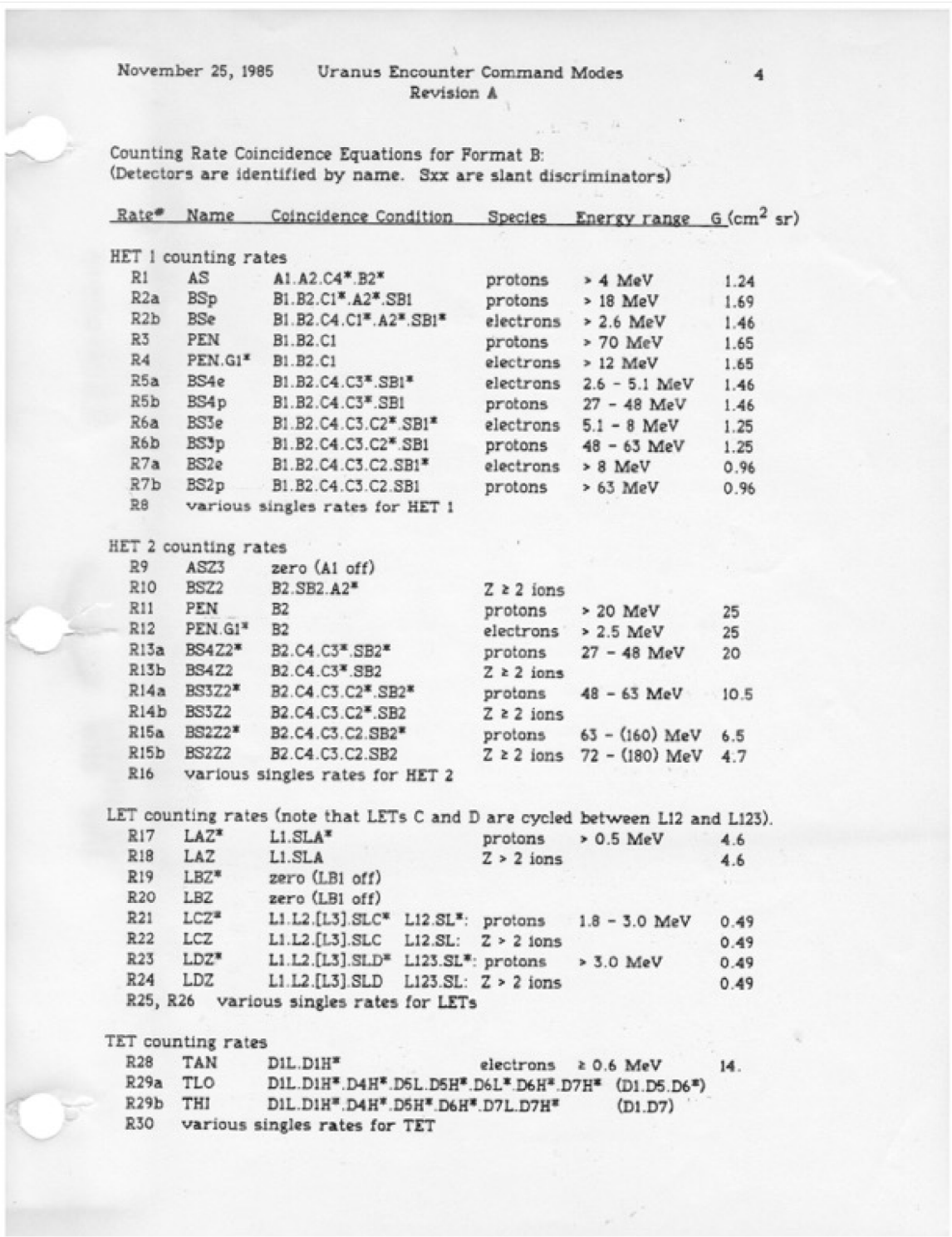


Figure 18. HET 1 singles rates at Neptune, scanned plot and data as submitted.

Appendix C. Scanned Original Documents

This section contains scanned documents which were the original source for tables contained elsewhere in this document.

Figure 19



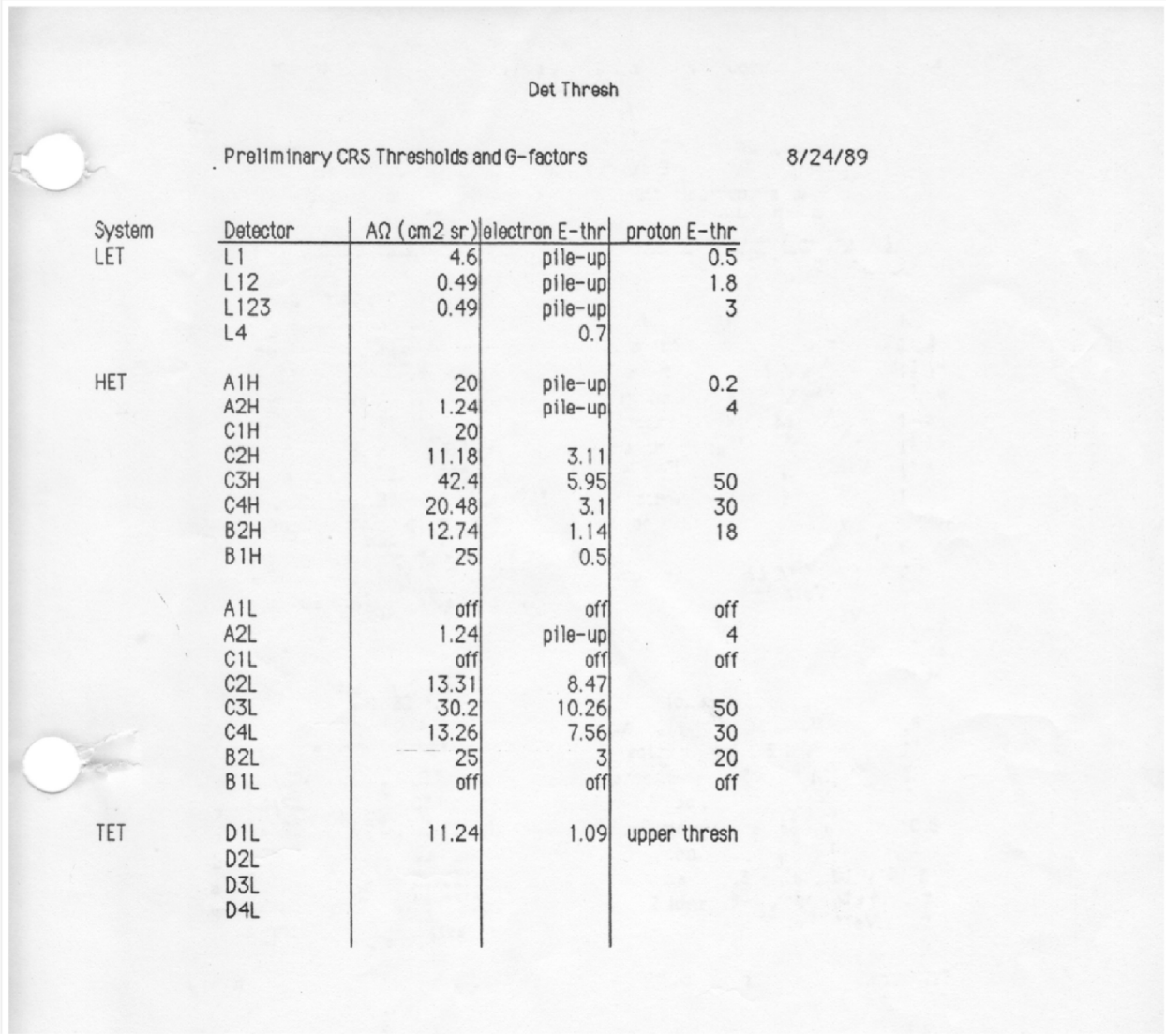
November 25, 1985 Uranus Encounter Command Modes 4
Revision A

Counting Rate Coincidence Equations for Format B:
(Detectors are identified by name. Sxx are slant discriminators)

Rate#	Name	Coincidence Condition	Species	Energy range	G (cm^2 sr)
HET 1 counting rates					
R1	AS	A1.A2.C4*.B2*	protons	> 4 MeV	1.24
R2a	BSp	B1.B2.C1*.A2*.SB1	protons	> 18 MeV	1.69
R2b	BSe	B1.B2.C4.C1*.A2*.SB1*	electrons	> 2.6 MeV	1.46
R3	PEN	B1.B2.C1	protons	> 70 MeV	1.65
R4	PEN.G1*	B1.B2.C1	electrons	> 12 MeV	1.65
R5a	BS4e	B1.B2.C4.C3*.SB1*	electrons	2.6 - 5.1 MeV	1.46
R5b	BS4p	B1.B2.C4.C3*.SB1	protons	27 - 48 MeV	1.46
R6a	BS3e	B1.B2.C4.C3.C2*.SB1*	electrons	5.1 - 8 MeV	1.25
R6b	BS3p	B1.B2.C4.C3.C2*.SB1	protons	48 - 63 MeV	1.25
R7a	BS2e	B1.B2.C4.C3.C2.SB1*	electrons	> 8 MeV	0.96
R7b	BS2p	B1.B2.C4.C3.C2.SB1	protons	> 63 MeV	0.96
R8	various singles rates for HET 1				
HET 2 counting rates					
R9	ASZ3	zero (A1 off)			
R10	BSZ2	B2.SB2.A2*	Z ≥ 2 ions		
R11	PEN	B2	protons	> 20 MeV	25
R12	PEN.G1*	B2	electrons	> 2.5 MeV	25
R13a	BS4Z2*	B2.C4.C3*.SB2*	protons	27 - 48 MeV	20
R13b	BS4Z2	B2.C4.C3*.SB2	Z ≥ 2 ions		
R14a	BS3Z2*	B2.C4.C3.C2*.SB2*	protons	48 - 63 MeV	10.5
R14b	BS3Z2	B2.C4.C3.C2*.SB2	Z ≥ 2 ions		
R15a	BS2Z2*	B2.C4.C3.C2.SB2*	protons	63 - (160) MeV	6.5
R15b	BS2Z2	B2.C4.C3.C2.SB2	Z ≥ 2 ions	72 - (180) MeV	4.7
R16	various singles rates for HET 2				
LET counting rates (note that LETs C and D are cycled between L12 and L123).					
R17	LAZ*	L1.SLA*	protons	> 0.5 MeV	4.6
R18	LAZ	L1.SLA	Z > 2 ions		4.6
R19	LBZ*	zero (LB1 off)			
R20	LBZ	zero (LB1 off)			
R21	LCZ*	L1.L2.[L3].SLC* L12.SL*:	protons	1.8 - 3.0 MeV	0.49
R22	LCZ	L1.L2.[L3].SLC L12.SL:	Z > 2 ions		0.49
R23	LDZ*	L1.L2.[L3].SLD* L123.SL*:	protons	> 3.0 MeV	0.49
R24	LDZ	L1.L2.[L3].SLD L123.SL:	Z > 2 ions		0.49
R25, R26	various singles rates for LETs				
TET counting rates					
R28	TAN	D1L.D1H*	electrons	≥ 0.6 MeV	14.
R29a	TLO	D1L.D1H*.D4H*.D5L.D5H*.D6L*.D6H*.D7H*		(D1.D5.D6*)	
R29b	THI	D1L.D1H*.D4H*.D5H*.D6H*.D7L.D7H*		(D1.D7)	
R30	various singles rates for TET				

Figure 19. Coincidence definitions and responses during the Uranus encounter. The table contained in this figure was the source for Table 3.

Figure 20



Det Thresh

Preliminary CRS Thresholds and G-factors 8/24/89

System	Detector	AΩ (cm2 sr)	electron E-thr	proton E-thr
LET	L1	4.6	pile-up	0.5
	L12	0.49	pile-up	1.8
	L123	0.49	pile-up	3
	L4		0.7	
HET	A1H	20	pile-up	0.2
	A2H	1.24	pile-up	4
	C1H	20		
	C2H	11.18	3.11	
	C3H	42.4	5.95	50
	C4H	20.48	3.1	30
	B2H	12.74	1.14	18
	B1H	25	0.5	
	A1L	off	off	off
	A2L	1.24	pile-up	4
	C1L	off	off	off
	C2L	13.31	8.47	
	C3L	30.2	10.26	50
	C4L	13.26	7.56	30
	B2L	25	3	20
	B1L	off	off	off
TET	D1L	11.24	1.09	upper thresh
	D2L			
	D3L			
	D4L			

Figure 20. Estimates of proton and electron responses of various single-detector countrates. The table contained in this figure was the source for Table 4.